

IBM Quantum Computers: Evolution, Performance, and Future Directions

Muhammad AbuGhanem^{1,2}

¹ Faculty of Science, Ain Shams University, Cairo, 11566, Egypt and

² Zewail City of Science, Technology and Innovation, Giza, 12678, Egypt*

(Dated: October 3, 2024)

Quantum computers represent a transformative frontier in computational technology, promising exponential speedups beyond classical computing limits. IBM Quantum has led significant advancements in both hardware and software, providing access to quantum hardware via IBM Cloud® since 2016, achieving a milestone with the world's first accessible quantum computer. This article explores IBM's quantum computing journey, focusing on the development of practical quantum computers. We summarize the evolution and advancements of IBM Quantum's processors across generations, including their recent breakthrough surpassing the 1,000-qubit barrier. The paper reviews detailed performance metrics across various hardware, tracing their evolution over time and highlighting IBM Quantum's transition from the noisy intermediate-scale quantum (NISQ) computing era towards fault-tolerant quantum computing capabilities.

Keywords: IBM Quantum computers, Superconducting quantum computers, performance of IBM's quantum computers, 1000-qubit processor, IBM quantum hardware, Heron, Condor, Qiskit, quantum utility.

I. INTRODUCTION

Quantum computers represent a revolutionary approach to computation [1], leveraging the principles of quantum mechanics [2, 3] to potentially solve problems that are beyond the reach of classical computers [4–7]. The NISQ era [8, 9] marks a pivotal phase in quantum computing, characterized by rapid advancements and challenges in achieving practical quantum applications [1].

Industry has been facilitating access to quantum computers for both academic and commercial users. Companies such as IBM (2016) [10], Rigetti Computing (2017) [11], IonQ (2020) [12], Honeywell (2020) [13], Google (2020) [14, 15], Xanadu (2020) [16], Oxford Quantum Circuits OQC (2021) [17], PASQAL (2022) [18], QuEra (2022) [19], and Quandela (2022) [20] have made their systems available via cloud platforms. While others have adopted a reseller model through web-based services [12, 21–23]. As a result, research on quantum computers has increased significantly [24]. For instance, scientific papers utilizing IBM's quantum systems via cloud service have reached approximately 2,800 as of February 2024, with over 3 trillion circuits executed through IBM Quantum platform [25].

IBM Quantum [26] has emerged as a key player in the quantum computing landscape, leading efforts to advance both quantum hardware and software capabilities. The development of scalable quantum processors based on superconducting qubits has been central to IBM Quantum's research and development efforts. Over the years, IBM has made significant strides in increasing qubit counts, improving qubit coherence times, and implementing error correction techniques necessary for reliable quantum computation [27, 28]. These advancements have posi-

tioned IBM Quantum as a leader in quantum computing research, with broad implications ranging from computational chemistry and optimization to cryptography and machine learning [27–32].

This paper explores IBM's journey in quantum computing, highlighting key technological achievements, current challenges, and future prospects. The study aims to present a comprehensive review of detailed performance metrics across IBM Quantum's quantum computers, crucial for historical documentation within the NISQ era literature. Metrics examined include relaxation times, qubit frequency and anharmonicity, readout assignment errors and readout length, single-qubit gate errors, connection errors, and gate times.

This paper is structured as follows: Section II provides an overview of IBM's quantum computing initiative. Section III examines the progression of IBM Quantum's hardware, detailing advancements from the 5-qubit *Canary* processor to breaking the 1,000-qubit barrier with *Condor* processor. Section IV summarizes the performance and characteristics of IBM's quantum computers, covering current systems, their capabilities, as well as retired systems and simulators. Moving to Section V, the focus shifts to IBM Quantum's software and tools. Section VI outlines IBM Quantum's roadmap and initiatives towards practical quantum computing, including their efforts in quantum safety. Finally, Section VII provides the conclusion.

II. IBM QUANTUM

A. Overview

IBM Quantum is a leading provider of quantum computing resources, offering access to top-of-the-line quantum hardware that is built with the latest technology to meet the needs of researchers, industry professionals, and developers.

* gaa1nem@gmail.com

IBM Quantum operates the most sophisticated collection of quantum systems globally, currently featuring seven utility-scale systems, with additional systems in development [33]. These systems are known for their exceptional reliability, boasting over 95% uptime collectively. They also demonstrate remarkable stability, with minimal fluctuations in two-qubit gate errors, which do not exceed 0.001 over periods spanning several months (median 2-qubit gate errors measured across all accessible *Eagle* processors from July 20 to September 20, 2023) [34, 35].

In 2023, IBM has introduced its latest quantum computing milestone with the unveiling of *Condor*, a quantum processor featuring 1,121 superconducting qubits arranged in a honeycomb configuration [36]. This follows the pattern set by earlier record-breaking machines such as *Eagle*, a 127-qubit chip launched in 2021 [34, 37, 38], and *Osprey*, a 433-qubit processor announced November 2022 [39, 40]. As part of its strategy, IBM also introduced a new quantum chip named *Heron*, boasting 133 qubits and achieving a remarkable record-low error rate that is three times lower than that of IBM’s previous quantum processor. This achievement marks a departure from IBM’s previous strategy of doubling qubit counts annually, signaling a shift towards prioritizing enhanced error resistance over further qubit scalability [28, 36].

IBM Quantum offers a wide range of hardware and software resources that support learning, experimentation, and collaboration in quantum computing [26, 41], with promising implications for accelerating scientific discovery, enhancing computational efficiency, and addressing complex real-world problems.

B. Breaking the 1,000-qubit barrier

IBM Quantum has introduced IBM *Condor*, a quantum processor with 1,121 superconducting qubits based on IBM Quantum’s cross-resonance gate technology [36]. *Condor* sets new standards in chip design (see Figure 1), featuring a 50% increase in qubit density, enhancements in qubit fabrication and laminate size, and over a mile of high-density cryogenic flex I/O wiring within a single dilution refrigerator.

Moving to high performing quantum processors, IBM Quantum introduced the first IBM Quantum *Heron* processor on the *ibm_torino* quantum system. Featuring 133 fixed-frequency qubits with tunable couplers. *Heron* delivers significant improvements in device performance (a 3-5x improvement in device performance) compared to IBM Quantum’s previous flagship 127-qubit *Eagle* processors [34, 37, 38], while virtually eliminating cross-talk. With *Heron*, IBM Quantum has developed qubit and gate technology that forms the foundation of IBM Quantum’s hardware roadmap moving forward [35].



FIG. 1: IBM’s latest quantum processor *Condor*, unveiled in 2023, features 1,121 superconducting qubits arranged in a honeycomb configuration. (Credit: Ryan Lavine, IBM).

C. IBM Quantum’s system two

IBM Quantum System Two serves as the foundation for scalable quantum computation and is currently operational at the IBM lab in Yorktown Heights, NY. Housing three IBM Quantum *Heron* processors, integrating cryogenic infrastructure with third-generation control electronics and classical runtime servers (see Figure 2). IBM Quantum System Two features a modular architecture designed to facilitate parallel circuit executions, which are essential for achieving quantum-centric supercomputing [35].

III. THE PROGRESSION OF IBM QUANTUM’S HARDWARE

IBM Quantum has developed several generations of quantum computers, each contributing to the advancement of quantum computing capabilities. These systems are built with cutting-edge superconducting quantum processors based on transmon qubits, chosen for their ability to offer control and scalability [42].

Processor types are categorized based on their technological attributes, identified by a combination of family and revision [43]. The term “family” (e.g., *Falcon*) denotes the potential circuit size and complexity achievable on the chip, primarily dictated by the number of qubits and their connectivity structure. “Revisions” (e.g., r1) signify different design variants within a specific family. These systems represent ongoing advancements in quantum computing hardware, supporting research and development in quantum algorithms and applications. In this section, we summarize the progression of IBM Quantum’s quantum processors.

A. Canary

The *Canary* family encompasses compact designs featuring between 5 and 16 qubits, utilizing an optimized 2D

TABLE I: Summary of the IBM Quantum's quantum processors and their progressions.

No.	Processor	Qubits ^a	QV	Revisions	Update	Date	Details
1	Canary	5-16	-	Canary r1	• The original r1 design introduced the <i>Canary</i> series with 5 qubits, integrating resonators and qubits on a single lithography layer, marking an initial step in advancing quantum computational capabilities.	January 2017	Sec. III A
				Canary r1.1	• Expanded the processor's capacity significantly, accommodating up to 16 qubits.		
				Canary r1.3	• Focused on a minimalist design featuring a single qubit, aimed at fundamental quantum computing research.		
2	Falcon	27	128	Falcon r1	• The first iteration in the <i>Falcon</i> series. Featuring a 28-qubit design with independent readout and utilizing a heavy-hexagonal connectivity graph optimized for cross-resonance two-qubit gates.	February 2020	Sec. III B
				Falcon r4	• Introduced multiplexed readout capabilities, improving qubit state readout efficiency compared to previous independent signal pathways		
				Falcon r5.10	• Pioneering advanced on-chip filtering methods that laid the groundwork for faster qubit state readouts in subsequent revisions.		
				Falcon r5.11	• Which improved qubit state readout speed through innovative on-chip filtering techniques. Such enhancements are pivotal for demonstrating quantum error correction and facilitating mid-circuit measurements.		
				Falcon r8	• Brought enhanced coherence properties, building upon the advancements of previous version		
3	Egret	33	512	Egret r1	• <i>Egret</i> applies tunable coupler advancements to a 33-qubit architecture, yielding in faster and more accurate (high-fidelity) two-qubit gates.	December 2022	Sec. III C
4	Hummingbird	65	128	Hummingbird r1	• Marked the initial endeavor to support a large number (>50) of qubits on a single chip.	October 2019	Sec. III D
				Hummingbird r2	• Leveraging improvements include readout multiplexing, efficient qubit-qubit couplers, and flip-chip technology.		
				Hummingbird r3	• A 65-qubit design with enhanced coherence properties.		
5	Eagle	127	128	Eagle r1	• Leveraging similar design elements and parameters as <i>Falcon</i> r5.11.	December 2021	Sec. III E
				Eagle r3	• Featuring a 127-qubit processor with enhanced coherence properties while maintaining design continuity with <i>Eagle</i> r1.		
6	Osprey	433	-	-	• The <i>Osprey</i> processor, setting new benchmarks in quantum computational power. <i>Osprey</i> incorporates enhanced device packaging technologies and custom flex cabling within the cryostat, enabling higher I/O capabilities within the same wiring footprint.	November 2022	Sec. III F
7	Heron	133-156	512	Heron r1	• This upgrade includes enhancements in signal delivery, utilizing high-density flex cabling to facilitate fast and high-fidelity control over both single-qubit and two-qubit operations.	December 2023	Sec. III G
				Heron r2	• The processor has been re-designed to combine 156 qubits in a heavy-hexagonal lattice. It also offers a new TLS mitigation capability that manages the chip's TLS environment, enhancing overall coherence and stability. Currently accessible through the <i>ibm_fez</i> quantum computer.		
8	Condor	1,121	-	-	• A quantum processor with 1,121 superconducting qubits based on IBM Quantum's cross-resonance gate technology. Condor marks a significant advancement in chip design, featuring a 50% increase in qubit density.	December 2023	Sec. III H

^a Maximum number.^b Value absent from the source.

lattice where all qubits and readout resonators reside on a single layer [43]. This family has seen several revisions aimed at refining and expanding its capabilities. The original r1 design (January 2017) introduced the *Canary* series with 5 qubits, integrating resonators and qubits on a single lithography layer, marking an initial step in advancing quantum computational capabilities. Building upon this, r1.1 (May 2017) expanded the processor's capacity, accommodating up to 16 qubits. r1.3 (December 2019), which focused on a minimalist design featuring a single qubit, aimed at fundamental quantum computing research [43].

B. Falcon

The *Falcon* family is tailored for medium-scale circuits, boasting a QV (quantum volume) of 128. It serves as a crucial testing ground for demonstrating performance enhancements and scalability improvements before integrating them into larger quantum devices. Native gates and operations supported by *Falcon* devices include CX, ID, DELAY, MEASURE, RESET, RZ, SX, X, IF_ELSE, FOR_LOOP, and SWITCH_CASE.

Within the *Falcon* family, several revisions have been

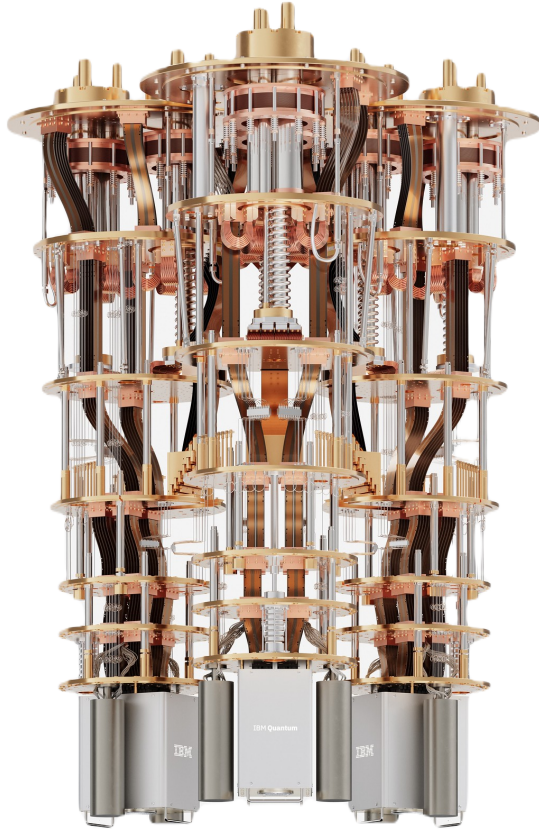


FIG. 2: IBM Quantum System Two, unveiled at the IBM Quantum Summit 2023, represents IBM's first modular quantum computer and serves as a foundational element in IBM's quantum-centric supercomputing architecture. (Image source: IBM Quantum).

developed to refine and expand its capabilities: The series commenced with *Falcon* r1 in February 2020, characterized by its 28-qubit design with independent readout and utilizing a heavy-hexagonal connectivity graph optimized for cross-resonance two-qubit gates. April 2020 saw the introduction of *Falcon* r4, which introduced multiplexed readout capabilities, improving qubit state readout efficiency compared to previous independent signal pathways. *Falcon* r5.10, released in December 2020, pioneering advanced on-chip filtering methods that laid the groundwork for faster qubit state readouts in subsequent revisions. This version also implemented space-saving “direct-couplers” to enhance qubit coupling efficiency, crucial for scaling quantum systems. *Falcon* r5.11, launched in January 2021, further improved qubit state readout speed through innovative on-chip filtering techniques, facilitating quantum error correction and mid-circuit measurements. In September 2021, the introduction of *Falcon* r8 brought enhanced coherence properties, building upon the advancements of previous versions [43].

C. Egret

The *Egret* quantum processor features a QV of 512 and introduces tunable couplers on a 33-qubit platform, significantly enhancing the speed and fidelity of two-qubit gates. In December 2022, IBM Quantum launched the first iteration of the *Egret* processor, designated as r1. It demonstrated the highest QV among IBM Quantum systems, marking substantial advancements in reducing two-qubit gate error rates. The *Egret* quantum processor delivers notable improvements in gate fidelity, with many gates achieving 99.9% fidelity, while also minimizing spectator errors [43].

D. Hummingbird

The *Hummingbird* family features a QV of 128 and utilizes a heavy-hexagonal qubit layout, accommodating up to 65 qubits. October 2019 marked the debut of *Hummingbird* r1, representing the initial effort to support a large number (>50) of qubits on a single chip, setting the stage for subsequent advancements in quantum processor design and scalability. August 2020 saw the release of *Hummingbird* r2, featuring 65 qubits and leveraging improvements, such as readout multiplexing, efficient qubit-qubit couplers, and flip-chip technology, which collectively enhance the scalability and operational capabilities of the *Hummingbird* family. In December 2021, *Hummingbird* r3 introduced a 65-qubit design with enhanced coherence properties, reflecting advancements in quantum processing stability and performance [43].

E. Eagle

The *Eagle* family boasts a QV of 128 and integrates advanced packaging technologies to accommodate 127 qubits [37]. These processors employ a heavy-hexagonal qubit layout, where qubits are connected to two or three neighbors, resembling the edges and corners of tessellated hexagons [38], see Figure 3. This layout minimizes errors from interactions between adjacent qubits, thereby enhancing processor reliability and functionality without compromising performance [34]. Native gates and operations supported include ECR, ID, DELAY, MEASURE, RESET, RZ, SX, X, IF_ELSE, FOR_LOOP, AND SWITCH_CASE.

In December 2021, *Eagle* r1 was introduced, leveraging similar design elements and parameters as *Falcon* r5.11. This version supports fast qubit readout and aims for comparable gate speeds and error rates [34]. In December 2022, *Eagle* r3 was released, featuring a 127-qubit processor with enhanced coherence properties while maintaining design continuity with *Eagle* r1 [43]. Currently, *Eagle* systems are deployed at various IBM Quantum's quantum computers. The error map and layout of a quantum

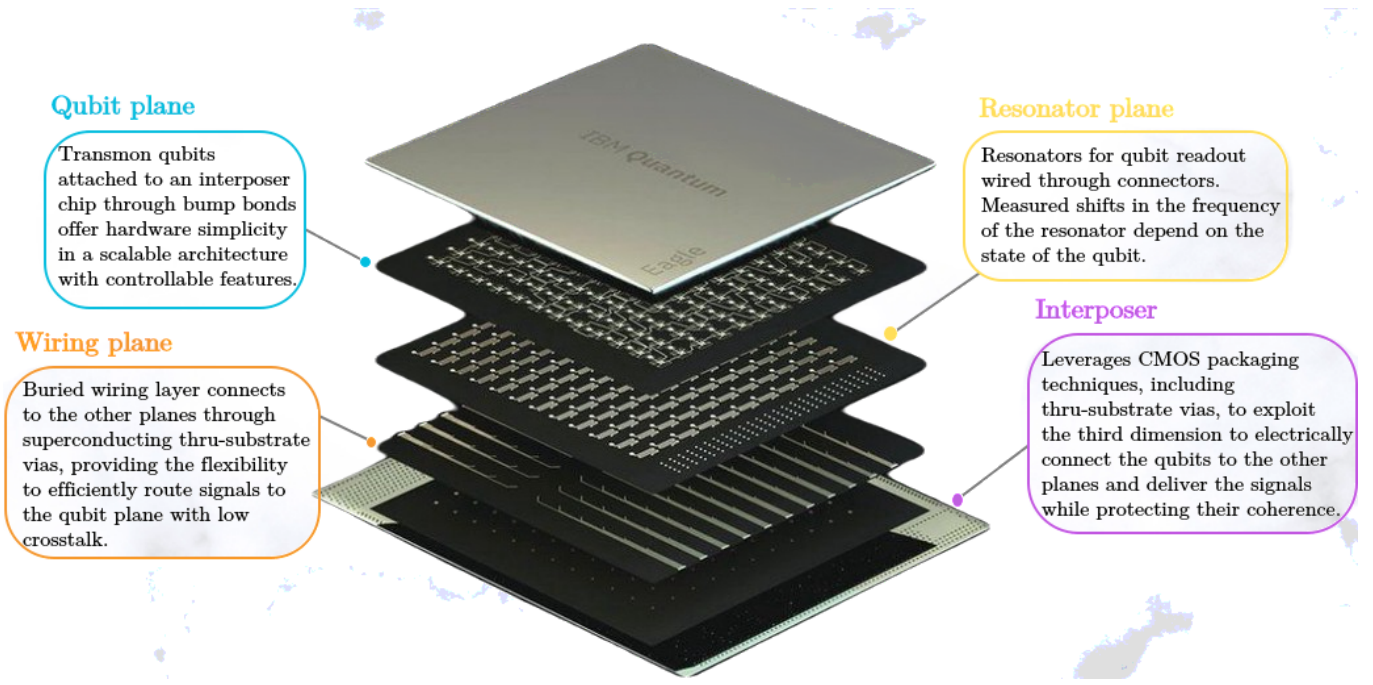


FIG. 3: IBM Quantum’s *Eagle* processors family configuration. These processors utilize a heavy-hexagonal qubit layout, where qubits connect with two or three neighboring qubits resembling edges and corners of tessellated hexagons. This design reduces errors caused by interactions between adjacent qubits, thereby improving processor reliability and functionality while maintaining high performance.

computer that is built based on an *Eagle* processor, such as *ibm_sherbrooke*, is depicted in Figure 4.

F. Osprey

The *Osprey* quantum processor boasting 433 qubits, nearly four times the size of its predecessor, *Eagle*. *Osprey* integrates enhanced device packaging technologies and custom flex cabling within the cryostat, enabling higher I/O capabilities within the same wiring footprint. IBM Quantum unveiled the *Osprey* processor in November 2022. *Osprey* has the potential to execute complex computations far surpassing the capabilities of classical computers. For context, the number of classical bits required to represent a single state on the IBM *Osprey* processor exceeds the total number of atoms in the observable universe [43].

G. Heron

Heron represents a significant advancement in quantum computing, featuring a QV of 512 and incorporating innovations in signal delivery previously seen in the *Osprey* processor. With 133 qubits, *Heron* builds upon the size and capabilities of its predecessor, *Egret*, and shares a similar footprint to *Eagle*. This upgrade includes enhancements in signal delivery, utilizing

high-density flex cabling to facilitate fast and high-fidelity control over both single-qubit and two-qubit operations. Native gates and operations supported by *Heron* include CZ, ID, DELAY, MEASURE, RESET, RZ, SX, X, IF_ELSE, FOR_LOOP, and SWITCH_CASE.

In December 2023, *Heron r1* was introduced, leveraging 133 qubits as the first version of *Heron*, currently accessible through *ibm_torino*. In July 2024, the processor has been re-designed to combine 156 qubits in a heavy-hexagonal lattice. It also offers a new TLS mitigation capability that manages the chip’s TLS environment, enhancing overall coherence and stability. The *Heron r2* processor, currently accessible through *ibm_fez* quantum computer [43].

H. Condor

In December 2023, IBM Quantum unveiled *Condor*, a groundbreaking quantum processor consists of 1,121 superconducting qubits and leveraging IBM Quantum’s cross-resonance gate technology [36, 44]. This technology facilitates precise two-qubit operations between superconducting qubits with fixed frequencies, known for their simplicity in implementation and resilience against noise [44].

Condor represents a leap forward in chip design, boasting a 50% increase in qubit density and notable enhancements in qubit fabrication and laminate size. Moreover,

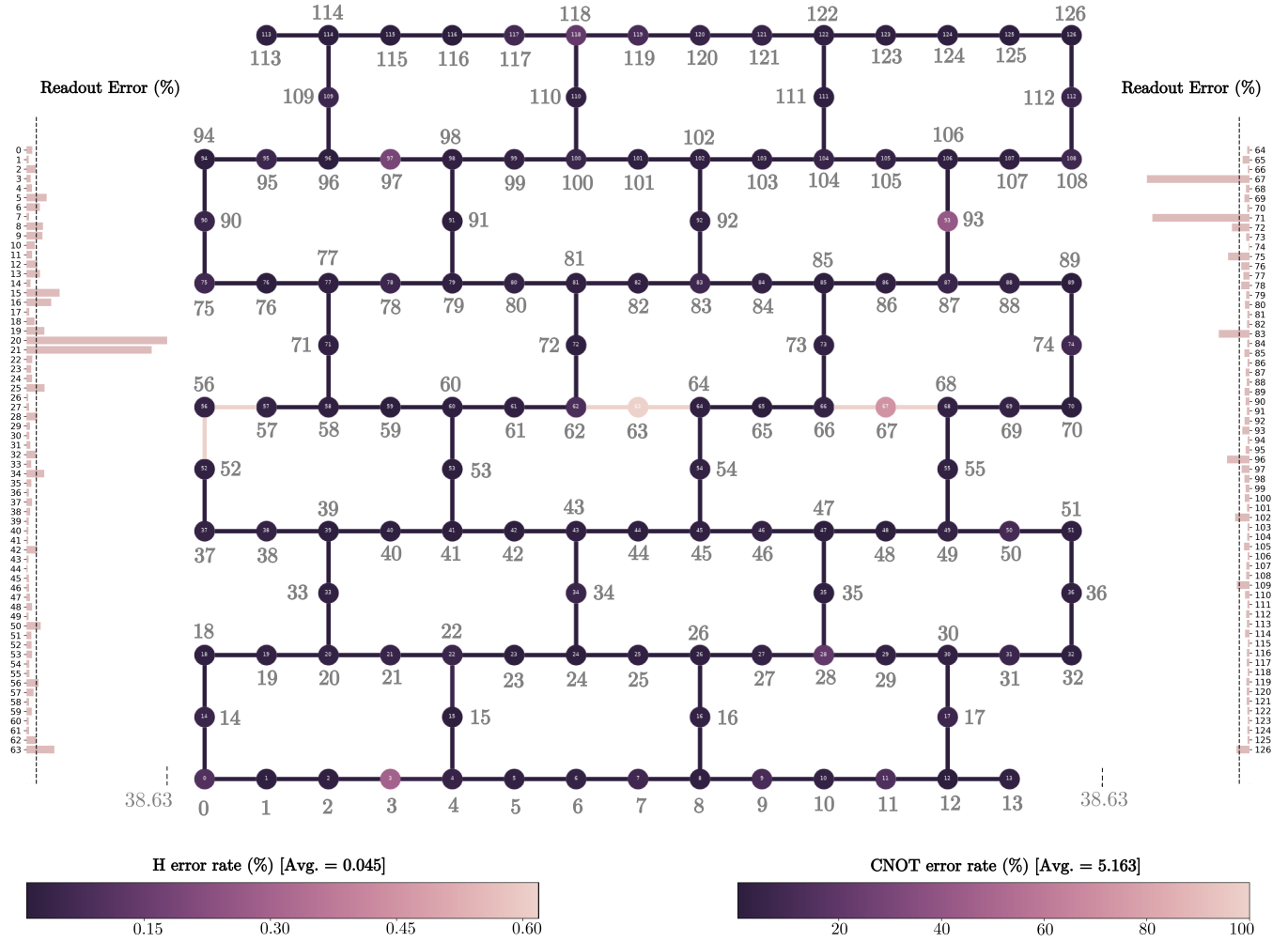


FIG. 4: Readout error map and layout of the *ibm_sherbrooke* quantum computer. This quantum system is based on an *Eagle r3* quantum processor, featuring 127 superconducting transmon qubits. Key performance metrics include median ECR error: 7.571×10^{-3} , median SX error: 2.411×10^{-4} median readout error: 1.350×10^{-2} median T1: $262.69 \mu\text{s}$, and median T2: $176.67 \mu\text{s}$, as of August 1, 2024.

it integrates an impressive length of over a mile of high-density cryogenic flex I/O wiring within a single dilution refrigerator. With performance comparable to its predecessor, the 433-qubit *Osprey*, *Condor* signifies a significant milestone in quantum computing innovation. It effectively tackles scalability challenges while offering valuable insights for future hardware designs [43].

IV. PERFORMANCE AND CHARACTERISTICS OF IBM'S QUANTUM COMPUTERS

A. Evolution of Quantum Systems

IBM Quantum's quantum computing offerings have evolved to include both current and retired systems. These systems range from early developments to advanced processors with up to 433 qubits (see Table II

for specific details). The journey from retired systems to the latest generations reflects IBM's continuous efforts to push the boundaries of quantum computation (see Table III). For a view of the availability and details of IBM Quantum's current quantum systems, including access plans, interested readers are referred to [45].

B. Retired systems and simulators

IBM's commitment to quantum computing is evident through a series of pioneering systems, some of which have since been retired. Systems such as *ibmq_5_yorktown* and *ibmq_16_melbourne*, retired on August 9, 2021. *ibmq_manhattan* followed on September 22, 2021, and earlier systems such as *ibmq_athens* and *ibmq_rome* were retired on June 30, 2021. Refer to Table II for a list of retired systems. These quantum systems, alongside quantum simulators, were pivotal in early

quantum algorithm experimentation and have paved the way for newer generations that continue to push the boundaries of quantum computing. Appendix A provides detailed performance summaries of these quantum computers, recorded for historical documentation in the NISQ computing era literature.

C. The up-to-date machines' performance

This section analyzes the performance metrics of 15 up-to-date IBM Quantum's quantum machines. Tables IV to XVIII summarize the hardware performance, qubit characteristics, and specifications of these quantum computers. Key parameters such as coherence times (T1 and T2), qubit frequencies, qubit anharmonicity, readout assignment error, readout length, qubit flip probabilities, as well as error rates for both single-qubit and two-qubit gates.

V. THE IBM QUANTUM'S SOFTWARE

A. Qiskit

Qiskit, the software development kit for quantum information science, launched by IBM in 2017 as an open-source toolbox for quantum computing. Over the past six years, it has flourished significantly. Qiskit has been installed over 6 million times, with current installations occurring at a rate of 300,000 per month [46]. Boasting more than 2,000 forks, over 8,000 contributions, and has facilitated the execution of over 3 trillion circuits [46]. By a significant margin, Qiskit stands out as the most widely-adopted quantum computing software [47].

Qiskit has demonstrated its effectiveness in recent studies in quantum computing, particularly in error mitigation [27]. Moreover, it played a crucial role in achieving fault-tolerant magic state preparation surpassing break-even fidelity [48], as well as in numerous significant studies involving up to 133 qubits and thousands of two-qubit entangling gates [49–64].

B. Qiskit patterns

Qiskit patterns, outline a structured four-step process for executing algorithms on quantum computers, aligning with its software architecture (shown in Figure 5). Initially, classical problems are translated into quantum computations by constructing circuits that encode the specific problem. Qiskit provides a user-friendly circuit construction API capable of handling extensive circuits. Subsequently, circuits undergo transformation—referred to as transpilation—to optimize them for execution on target hardware, focusing on circuit-to-circuit rewriting rather than full compilation to classical controller instructions. Following transpilation, circuits are executed

on a target backend using primitive computations. Finally, the obtained results are post-processed to derive solutions for the original problem.

Workflows may iterate through these steps, incorporating advanced patterns like generating new circuits based on results from prior batches [65], integrating quantum and classical computing in a quantum-centric supercomputing architecture [66, 67]. Complex pattern orchestration is streamlined via the Qiskit serverless framework [68].

C. Qiskit circuits

Quantum circuits are central to Qiskit's architecture, representing computations as sequences of instructions that can be manipulated and analyzed within the software. Qiskit defines circuits broadly, encompassing operations on both quantum and classical data. This includes standard actions like qubit operations and measurements, as well as advanced mathematical operators such as unitaries, Cliffords, isometries, and Fourier transforms. Circuits may also involve classical computations in real-time, such as applying Boolean functions to measurement outcomes, and classical control flow mechanisms like loops and branches.

Circuits can also delineate timing operations and continuous-time qubit dynamics (CTQD) using pulse-defined gates. These levels of abstraction can be combined within a single circuit, facilitating modular composition. Figure 5 provides an overview of Qiskit's architecture, highlighting its components and interactions, while Figure 6 illustrates diverse circuit types supported by Qiskit [46]. This flexibility supports the exploration of various quantum algorithms and physical implementations.

D. Scale to large numbers of qubits

In quantum computing, advancing in the field requires tackling utility-scale tasks, which involve computations on a significantly larger scale. This entails working with circuits that utilize more than 100 qubits and incorporate over 1000 gates.

To demonstrate large-scale operations on IBM Quantum systems, we consider the following example, involving the generation and analysis of a 100-qubit GHZ state ($|\text{GHZ}\rangle_{100} = \frac{1}{\sqrt{2}}(|0\rangle^{\otimes 100} + |1\rangle^{\otimes 100})$) [69]. This approach leverages the Qiskit patterns workflow and concludes with the measurement of the expectation value $\langle Z_0 Z_i \rangle$ for each qubit. The process of developing a quantum program using Qiskit entails four essential steps: mapping the problem to a quantum-native format, optimizing circuits and operators, executing with a quantum primitive function, and analyzing the resulting data.

TABLE II: List of IBM Quantum’s retired quantum systems and cloud simulators. Older systems are identified with names starting with “ibmq,” while newer systems use names beginning with “ibm.”

IBM Quantum quantum computers							
No.	Quantum System	Qubit count	Retirement date	No.	Quantum System	Qubit count	Retirement date
1	ibm.algiers	27	April 30, 2024	25	ibmq_bogota	5	June 17, 2022
2	ibm_cairo	27	April 30, 2024	26	ibmq_santiago	5	June 17, 2022
3	ibm_hanoi	27	April 30, 2024	27	ibmq_casablanca	7	March 2, 2022
4	ibmq_kolkata	27	April 1, 2024	28	ibmq_sydney	27	January 11, 2022
5	ibmq_mumbai	27	April 1, 2024	29	ibmq_dublin	27	November 16, 2021
6	ibm_ithaca	65	January 24, 2024	30	ibmq_manhattan	65	September 22, 2021
7	ibm_nairobi	7	November 28, 2023	31	ibmq_5_yorktown	5	August 9, 2021
8	ibm_lagos	7	November 28, 2023	32	ibmq_16_melbourne	15	August 9, 2021
9	ibm_perth	7	November 28, 2023	33	ibmq_paris	27	June 30, 2021
10	ibm_auckland	27	November 9, 2023	34	ibmq_rome	5	June 30, 2021
11	ibmq_guadalupe	16	October 27, 2023	35	ibmq_athens	5	June 30, 2021
12	ibmq_lima	5	September 26, 2023	36	ibmq_berlin	27	December 31, 2020
13	ibmq_belem	5	September 26, 2023	37	ibmq_boeblingen	20	January 31, 2021
14	ibmq_quito	5	September 26, 2023	38	ibmq_ourense	5	January 15, 2021
15	ibmq_manila	5	September 26, 2023	39	ibmq_vigo	5	January 15, 2021
16	ibmq_jakarta	7	September 26, 2023	40	ibmq_valencia	5	January 15, 2021
17	ibm_seattle	433	September 7, 2023	41	ibmq_rochester	53	October 31, 2020
18	ibm_washington	127	June 3, 2023	42	ibmq_cambridge	28	October 31, 2020
19	ibmq_oslo	7	May 4, 2023	43	ibmq_almaden	20	August 31, 2020
20	ibmq_geneva	27	May 4, 2023	44	ibmq_singapore	20	August 31, 2020
21	ibmq_montreal	27	April 11, 2023	45	ibmq_johannesburg	20	August 31, 2020
22	ibmq_toronto	27	April 11, 2023	46	ibmq_essex	5	August 31, 2020
23	ibmq_armonk	1	July 7, 2022	47	ibmq_burlington	5	August 31, 2020
24	ibmq_brooklyn	65	June 28, 2022	48	ibmq_london	5	August 31, 2020

IBM Quantum cloud simulators							
No.	Quantum simulators	Qubit counts	Processor type				Retirement date
1	simulator_stabilizer	5000	Clifford simulator			-	May 15, 2024
2	simulator_mps	100	Matrix product state			-	May 15, 2024
3	simulator_extended_stabilizer	63	Extended Clifford (e.g. Clifford+T)			-	May 15, 2024
4	ibmq_qasm_simulator	32	General, context-aware			-	May 15, 2024
5	simulator_statevector	32	Schrödinger wavefunction			-	May 15, 2024

TABLE III: The up-to-date IBM Quantum’s quantum computers.

No.	System	Qubits	QV	EPLG ^a	CLOPS ^b	T1 (μs) ^c	T2 (μs) ^c	QPU ^d	Processor	Version	Features	Performance
1	ibm_fez	156	512	0.8%	3.8K	136.52	78.58	us-east	Heron r1	1.0.0	OpenQASM 3	Table IV
2	ibm_toronto	133	512	1.0%	3.8K	158.27	122.18	us-east	Heron r1	1.0.22	OpenQASM 3	Table V
3	ibm_kyiv	127	128	1.8%	5.0K	257.27	111.01	us-east	Eagle r3	1.20.12	OpenQASM 3	Table VI
4	ibm_sherbrooke	127	128	1.8%	5.0K	275.67	190.58	us-east	Eagle r3	1.5.3	OpenQASM 3	Table VII
5	ibm_quebec	127	128	2.2%	5.0K	295.08	161.68	us-east	Eagle r3	1.2.8	OpenQASM 3	Table IX
6	ibm_brisbane	127	128	2.2%	5.0K	225.28	144.34	us-east	Eagle r3	1.1.33	OpenQASM 3	Table VIII
7	ibm_rensselaer	127	128	2.6%	5.0K	262.14	176.61	us-east	Eagle r3	1.1.6	OpenQASM 3	Table XI
8	ibm_brussels	127	128	2.7%	5.0K	293.28	160.86	us-east	Eagle r3	1.1.13	OpenQASM 3	Table X
9	ibm_kawasaki	127	128	3.0%	5.0K	197.23	142.23	us-east	Eagle r3	2.1.31	OpenQASM 3	Table XIII
10	ibm_strasbourg	127	128	3.0%	5.0K	269.01	169.50	eu-de	Eagle r3	1.0.10	OpenQASM 3	Table XV
11	ibm_nazca	127	128	3.5%	5.0K	178.17	110.34	us-east	Eagle r3	1.0.31	OpenQASM 3	Table XIV
12	ibm_kyoto	127	128	3.6%	5.0K	216.88	93.31	us-east	Eagle r3	1.2.38	OpenQASM 3	Table XII
13	ibm_osaka	127	128	3.6%	5.0K	278.37	132.37	us-east	Eagle r3	1.1.8	OpenQASM 3	Table XVI
14	ibm_cleveland	127	128	5.0%	5.0K	213.58	191.65	us-east	Eagle r3	1.5.1	OpenQASM 3	Table XVII
15	ibm_cusco	127	128	6.8%	5.0K	135.76	72.35	us-east	Eagle r3	1.0.40	OpenQASM 3	Table XVIII

^a Error per layered gate for a 100-qubit chain.

^b Hardware-aware circuit layer operations per second.

^c The median values of the relaxation time-T1 and the coherence time-T2, measured in microseconds (μs). Accessed July 2, 2024.
except for the *ibm_fez* accessed 04 July 2024. Most systems support a maximum of 300 circuits and 100,000 shots.

^d QPU region.

TABLE IV: Summary of hardware performance, qubit characteristics, and key specifications for the 156 qubit quantum computer *ibm_fez*. The basis gates employed by this system are CZ, ID, RZ, SX, and X. The processor type is *Heron r2* (version 1.0.0). As of July 4, 2024, the system demonstrates a median CZ error of 2.848×10^{-3} , and a median gate time of 68 ns.

System parameters	Mean	StDev	Min	1 st Quartile	Median	3 rd Quartile	Max
T1 (μ s)	137.558138	47.587586	13.834783	106.863088	136.523081	162.444316	271.626108
T2 (μ s)	82.612083	46.241133	4.583184	52.180838	78.580919	111.299718	268.217025
Frequency (GHz)	0.0	0.0	0.0	0.0	0.0	0.0	0.0
Anharmonicity (GHz)	0.0	0.0	0.0	0.0	0.0	0.0	0.0
Readout assignment error	0.024617	0.033318	0.003100	0.008325	0.016300	0.032025	0.363200
Prob. measure $ 0\rangle$ prepare $ 1\rangle$	0.029385	0.038514	0.0	0.011650	0.020000	0.035050	0.416400
Prob. measure $ 1\rangle$ prepare $ 0\rangle$	0.019849	0.029431	0.0	0.004400	0.012700	0.026617	0.310000
Readout length (ns)	1560	0.0	1560	1560	1560	1560	1560
ID error	0.000443	0.000589	0.000129	0.000232	0.000288	0.000398	0.005070
The Z-axis rotation (R_Z) error	0.0	0.0	0.0	0.0	0.0	0.0	0.0
The \sqrt{X} (SX) error	0.000443	0.000589	0.000129	0.000232	0.000288	0.000398	0.005070
Pauli-X error	0.000443	0.000589	0.000129	0.000232	0.000288	0.000398	0.005070

TABLE V: Summary of hardware performance, qubit characteristics, and key specifications for the 133 qubit quantum computer *ibm_torino*. The basis gates of this machine are CZ, ID, RZ, SX, and X. The processor type is *Heron r1* (version 1.0.22). As of July 3, 2024, the system demonstrates a median CZ error of 4.769×10^{-3} , and a median gate time of 84 ns.

System parameters	Mean	StDev	Min	1 st Quartile	Median	3 rd Quartile	Max
T1 (μ s)	157.481331	71.344649	10.161401	103.099556	162.909929	215.918228	320.890662
T2 (μ s)	131.875390	65.751564	14.347368	81.995644	129.917339	175.014680	314.087388
Frequency (GHz)	0.0	0.0	0.0	0.0	0.0	0.0	0.0
Anharmonicity (GHz)	0.0	0.0	0.0	0.0	0.0	0.0	0.0
Readout assignment error	0.030614	0.043730	0.005100	0.011900	0.020500	0.036600	0.433300
Prob. measure $ 0\rangle$ prepare $ 1\rangle$	0.036508	0.067759	0.003333	0.013600	0.022000	0.041200	0.716200
Prob. measure $ 1\rangle$ prepare $ 0\rangle$	0.024720	0.026747	0.002200	0.008400	0.015400	0.033200	0.187000
Readout length (ns)	1560	0.0	1560	1560	1560	1560	1560
ID error	0.000754	0.001624	0.000112	0.000241	0.000317	0.000542	0.013031
The Z-axis rotation (R_Z) error	0.0	0.0	0.0	0.0	0.0	0.0	0.0
The \sqrt{X} (SX) error	0.000754	0.001624	0.000112	0.000241	0.000317	0.000542	0.013031
Pauli-X error	0.000754	0.001624	0.000112	0.000241	0.000317	0.000542	0.013031

TABLE VI: Summary of hardware performance, qubit characteristics, and key specifications for the 127-qubit quantum computer *ibm_kyiv*. The basis gates employed by this system include ECR, RZ, SX, ID, and X. The processor type is *Eagle r3* (version 1.20.12). As of July 3, 2024, the system demonstrates a median ECR error of 1.160×10^{-2} , and a median gate time of 561.778 ns.

System parameters	Mean	StDev	Min	1 st Quartile	Median	3 rd Quartile	Max
T1 (μ s)	263.380990	94.540378	25.637671	209.55451	254.456028	320.062960	576.494856
T2 (μ s)	146.828103	114.200863	13.236858	57.008413	110.193349	195.220693	495.328304
Frequency (GHz)	4.619478	0.112134	4.341284	4.540540	4.612760	4.702569	4.958907
Anharmonicity (GHz)	0.0	0.0	0.0	0.0	0.0	0.0	0.0
Readout assignment error	0.015976	0.033548	0.001100	0.003450	0.006900	0.012800	0.323000
Prob. measure $ 0\rangle$ prepare $ 1\rangle$	0.017805	0.033056	0.001200	0.005200	0.009000	0.015600	0.287800
Prob. measure $ 1\rangle$ prepare $ 0\rangle$	0.014146	0.036527	0.0	0.001300	0.004000	0.010200	0.358200
Readout length (ns)	1244.444	0.0	1244.444	1244.444	1244.444	1244.444	1244.444
ID error	0.000549	0.001485	0.000105	0.000194	0.000293	0.000517	0.016190
The Z-axis rotation (R_Z) error	0.0	0.0	0.0	0.0	0.0	0.0	0.0
The \sqrt{X} (SX) error	0.000549	0.001485	0.000105	0.000194	0.000293	0.000517	0.016190
Pauli-X error	0.000549	0.001485	0.000105	0.000194	0.000293	0.000517	0.016190

TABLE VII: Summary of hardware performance, qubit characteristics, and key specifications for the 127-qubit quantum computer *ibm_sherbrooke*. The basis gates employed by this system include ECR, RZ, SX, ID, and X. The processor type is Eagle r3 (version 1.5.3). As of July 3, 2024, the system demonstrates a median ECR error of 7.400×10^{-3} , and a median gate time of 533.333 ns.

System parameters	Mean	StDev	Min	1 st Quartile	Median	3 rd Quartile	Max
T1 (μ s)	274.123442	98.517950	21.158141	224.50857	269.502295	344.268918	521.784547
T2 (μ s)	189.105523	122.86363	12.393942	79.646051	183.988935	263.367610	725.093616
Frequency (GHz)	4.789996	0.109104	4.455281	4.731590	4.794027	4.859388	5.057532
Anharmonicity (GHz)	-0.310393	0.005480	-0.324263	-0.312253	-0.310932	-0.309626	-0.271864
Readout assignment error	0.028869	0.058722	0.002800	0.007900	0.012200	0.023600	0.439200
Prob. measure $ 0\rangle$ prepare $ 1\rangle$	0.033345	0.070388	0.003200	0.008400	0.013400	0.024300	0.483333
Prob. measure $ 1\rangle$ prepare $ 0\rangle$	0.024393	0.054051	0.001200	0.005500	0.009400	0.020500	0.447600
Readout length (ns)	1244.444	0.0	1244.444	1244.444	1244.444	1244.444	1244.444
ID error	0.000441	0.000791	0.000080	0.000167	0.000227	0.000349	0.006187
The Z-axis rotation (R_Z) error	0.0	0.0	0.0	0.0	0.0	0.0	0.0
The \sqrt{X} (SX) error	0.000441	0.000791	0.000080	0.000167	0.000227	0.000349	0.006187
Pauli-X error	0.000441	0.000791	0.000080	0.000167	0.000227	0.000349	0.006187

TABLE VIII: Summary of hardware performance, qubit characteristics, and key specifications for the 127-qubit quantum computer *ibm_brisbane*. The basis gates employed by this system include ECR, RZ, SX, ID, and X. The processor type is *Eagle* r3 (version 1.1.33). As of July 3, 2024, the system demonstrates a median ECR error of 8.335×10^{-3} , and a median gate time of 660 ns.

System parameters	Mean	StDev	Min	1 st Quartile	Median	3 rd Quartile	Max
T1 (us)	215.546208	79.938473	23.612698	151.804061	222.649128	266.129216	407.872593
T2 (us)	153.564636	82.301519	14.358729	90.089787	145.556518	218.296065	326.660536
Frequency (GHz)	4.896177	0.109272	4.609657	4.821185	4.905596	4.971761	5.117739
Anharmonicity (GHz)	-0.308664	0.005384	-0.359055	-0.309744	-0.308420	-0.307402	-0.289806
Readout assignment error	0.028724	0.046723	0.004000	0.008900	0.014100	0.023850	0.338500
Prob. measure $ 0\rangle$ prepare $ 1\rangle$	0.029354	0.044149	0.004600	0.009700	0.015600	0.024500	0.351000
Prob. measure $ 1\rangle$ prepare $ 0\rangle$	0.028094	0.059044	0.002400	0.007300	0.010800	0.020900	0.481000
Readout length (ns)	1300.00	0.0	1300.00	1300.00	1300.00	1300.00	1300.00
ID error	0.000689	0.003614	0.000077	0.000185	0.000244	0.000363	0.040644
The Z-axis rotation (R_Z) error	0.0	0.0	0.0	0.0	0.0	0.0	0.0
The \sqrt{X} (SX) error	0.000689	0.003614	0.000077	0.000185	0.000244	0.000363	0.040644
Pauli-X error	0.000689	0.003614	0.000077	0.000185	0.000244	0.000363	0.040644

TABLE IX: Summary of hardware performance, qubit characteristics, and key specifications for the 127-qubit quantum computer *ibm_quebec*. The basis gates of this machine are ECR, RZ, SX, ID, X. The processor type is *Eagle* r3 (version 1.2.8). As of July 3, 2024, the system demonstrates a median ECR error of 8.017×10^{-3} , and a median gate time of 593 ns.

System parameters	Mean	StDev	Min	1 st Quartile	Median	3 rd Quartile	Max
T1 (us)	292.051452	112.235331	3.180864	214.685833	288.916307	358.436905	616.631699
T2 (us)	178.416351	135.865063	2.208681	65.975403	145.882121	278.439621	583.406553
Frequency (GHz)	4.910363	0.113470	4.634752	4.831137	4.901556	4.996106	5.198909
Anharmonicity (GHz)	-0.298732	0.054194	-0.329975	-0.309970	-0.308308	-0.307014	0.0
Readout assignment error	0.041901	0.079884	0.002600	0.008050	0.013000	0.028300	0.484700
Prob. measure $ 0\rangle$ prepare $ 1\rangle$	0.040815	0.082489	0.002800	0.008700	0.013200	0.024700	0.470200
Prob. measure $ 1\rangle$ prepare $ 0\rangle$	0.042986	0.089180	0.001000	0.006800	0.012400	0.027200	0.522000
Readout length (ns)	835.555556	0.0	835.555556	835.555556	835.555556	835.555556	835.555556
ID error	0.002031	0.018074	0.000088	0.000171	0.000225	0.000345	0.203685
The Z-axis rotation (R_Z) error	0.0	0.0	0.0	0.0	0.0	0.0	0.0
The \sqrt{X} (SX) error	0.002031	0.018074	0.000088	0.000171	0.000225	0.000345	0.203685
Pauli-X error	0.002031	0.018074	0.000088	0.000171	0.000225	0.000345	0.203685

TABLE X: Summary of hardware performance, qubit characteristics, and key specifications for the 127-qubit quantum computer *ibm-brussels*. The basis gates employed by this system include ECR, RZ, SX, ID, and X. The processor type is *Eagle r3* (version 1.1.13). As of July 3, 2024, the system demonstrates a median ECR error of 8.074×10^{-3} , and a median gate time of 660 ns.

System parameters	Mean	StDev	Min	1 st Quartile	Median	3 rd Quartile	Max
T1 (μ s)	320.440117	111.234768	39.414051	246.872003	313.847394	389.887420	608.989954
T2 (μ s)	167.756680	117.414095	0.455292	65.949763	173.149154	243.485123	465.689813
Frequency (GHz)	4.800165	0.114353	4.532232	4.731179	4.798645	4.884004	5.074872
Anharmonicity (GHz)	-0.299139	0.055095	-0.380843	-0.310694	-0.309003	-0.307563	0.0
Readout assignment error	0.028740	0.033565	0.004800	0.010300	0.017200	0.034150	0.206667
Prob. measure $ 0\rangle$ prepare $ 1\rangle$	0.025434	0.031165	0.003400	0.010000	0.015400	0.029700	0.230000
Prob. measure $ 1\rangle$ prepare $ 0\rangle$	0.032045	0.042137	0.002600	0.010000	0.017000	0.037600	0.333600
Readout length (ns)	1600	0.0	1600	1600	1600	1600	1600
ID error	0.000387	0.000543	0.000086	0.000177	0.000242	0.000352	0.004047
The Z-axis rotation (R_Z) error	0.0	0.0	0.0	0.0	0.0	0.0	0.0
The \sqrt{X} (SX) error	0.000387	0.000543	0.000086	0.000177	0.000242	0.000352	0.004047
Pauli-X error	0.000387	0.000543	0.000086	0.000177	0.000242	0.000352	0.004047

TABLE XI: Summary of hardware performance, qubit characteristics, and key specifications for the 127-qubit quantum computer, *ibm-rensselaer*. The basis gates employed by this system include ECR, RZ, SX, ID, and X. The processor type is *Eagle r3* (version 1.1.6). As of July 3, 2024, this quantum system exhibits a median ECR error: 7.580×10^{-3} , and a median gate time of 665.889 ns.

System parameters	Mean	StDev	Min	1 st Quartile	Median	3 rd Quartile	Max
T1 (μ s)	259.126834	101.960836	22.517959	193.211648	261.637128	329.469093	502.305781
T2 (μ s)	176.992496	102.018513	0.954730	94.366764	172.220393	253.475846	470.735523
Frequency (GHz)	4.836538	0.116574	4.544908	4.763693	4.830515	4.919746	5.220783
Anharmonicity (GHz)	-0.288692	0.075452	-0.347815	-0.309668	-0.308135	-0.306593	0.0
Readout assignment error	0.021865	0.035818	0.002300	0.005550	0.008400	0.015600	0.199000
Prob. measure $ 0\rangle$ prepare $ 1\rangle$	0.022471	0.037413	0.002400	0.006400	0.009200	0.018900	0.207000
Prob. measure $ 1\rangle$ prepare $ 0\rangle$	0.021258	0.039389	0.001400	0.004100	0.007200	0.016200	0.244400
Readout length (ns)	1112.889	0.0	1112.889	1112.889	1112.889	1112.889	1112.889
ID error	0.000995	0.005936	0.000102	0.000165	0.000230	0.000336	0.065202
The Z-axis rotation (R_Z) error	0.0	0.0	0.0	0.0	0.0	0.0	0.0
The \sqrt{X} (SX) error	0.000995	0.005936	0.000102	0.000165	0.000230	0.000336	0.065202
Pauli-X error	0.000995	0.005936	0.000102	0.000165	0.000230	0.000336	0.065202

TABLE XII: Summary of hardware performance, qubit characteristics, and key specifications for the 127-qubit quantum computer *ibm-kyoto*. The basis gates employed by this system include ECR, RZ, SX, ID, and X. The processor type is *Eagle r3* (version 1.2.38). As of July 3, 2024, the system demonstrates a median ECR error of 1.023×10^{-2} , and a median gate time of 660 ns.

System parameters	Mean	StDev	Min	1 st Quartile	Median	3 rd Quartile	Max
T1 (μ s)	223.401174	70.329045	0.868321	179.834966	216.880493	261.150818	425.219660
T2 (μ s)	116.498508	81.507892	5.093271	50.531352	98.471325	164.392541	348.377179
Frequency (GHz)	4.966616	0.130136	4.704558	4.857412	4.959635	5.066503	5.250633
Anharmonicity (GHz)	-0.292802	0.065494	-0.312095	-0.308707	-0.307325	-0.305526	0.0
Readout assignment error	0.036971	0.052227	0.004600	0.009650	0.016400	0.041800	0.315300
Prob. measure $ 0\rangle$ prepare $ 1\rangle$	0.037713	0.064612	0.004000	0.009600	0.014400	0.039400	0.493400
Prob. measure $ 1\rangle$ prepare $ 0\rangle$	0.036229	0.047338	0.002800	0.008600	0.017000	0.046300	0.305600
Readout length (ns)	1400	0.0	1400	1400	1400	1400	1400
ID error	0.003028	0.022267	0.000106	0.000194	0.000289	0.000526	0.246250
The Z-axis rotation (R_Z) error	0.0	0.0	0.0	0.0	0.0	0.0	0.0
The \sqrt{X} (SX) error	0.003028	0.022267	0.000106	0.000194	0.000289	0.000526	0.246250
Pauli-X error	0.003028	0.022267	0.000106	0.000194	0.000289	0.000526	0.246250

TABLE XIII: Summary of hardware performance, qubit characteristics, and key specifications for the 127-qubit quantum computer *ibm_kawasaki*. The basis gates employed by this system include ECR, RZ, SX, ID, and X. The processor type is *Eagle r3* (version 2.1.31). As of July 3, 2024, the system demonstrates a median ECR error of 7.114×10^{-3} , and a median gate time of 586.667 ns.

System parameters	Mean	StDev	Min	1 st Quartile	Median	3 rd Quartile	Max
T1 (μ s)	195.343472	64.693363	0.776066	148.57249	196.852003	239.485612	344.118089
T2 (μ s)	160.814823	90.323244	6.473055	94.779526	148.271693	223.492753	502.659788
Frequency (GHz)	5.241257	0.130815	4.904341	5.156160	5.239658	5.340298	5.583662
Anharmonicity (GHz)	-0.301599	0.011852	-0.365607	-0.304317	-0.302589	-0.300511	-0.206400
Readout assignment error	0.028137	0.050709	0.004600	0.008050	0.010700	0.020500	0.383600
Prob. measure $ 0\rangle$ prepare $ 1\rangle$	0.024430	0.031478	0.004000	0.008900	0.012400	0.022600	0.206667
Prob. measure $ 1\rangle$ prepare $ 0\rangle$	0.031844	0.079804	0.002200	0.006700	0.009200	0.020400	0.730400
Readout length (ns)	1112.889	0.0	1112.889	1112.889	1112.889	1112.889	1112.889
ID error	0.000320	0.000330	0.000114	0.000170	0.000247	0.000328	0.003243
The Z-axis rotation (R_Z) error	0.0	0.0	0.0	0.0	0.0	0.0	0.0
The \sqrt{X} (SX) error	0.000320	0.000330	0.000114	0.000170	0.000247	0.000328	0.003243
Pauli-X error	0.000320	0.000330	0.000114	0.000170	0.000247	0.000328	0.003243

TABLE XIV: Summary of hardware performance, qubit characteristics, and key specifications for the 127-qubit quantum computer *ibm_nazca*. The basis gates employed by this system include ECR, RZ, SX, ID, and X. The processor type is *Eagle r3* (version 1.0.31). As of July 3, 2024, the system demonstrates a median ECR error of 1.240×10^{-2} , and a median gate time of 660 ns.

System parameters	Mean	StDev	Min	1 st Quartile	Median	3 rd Quartile	Max
T1 (μ s)	185.190222	69.655015	32.25129	140.13869	178.168265	233.203341	352.943675
T2 (μ s)	123.274041	78.552897	1.046602	61.592155	110.340019	176.435465	376.598767
Frequency (GHz)	5.080864	0.127984	4.769237	5.002285	5.081721	5.169752	5.382887
Anharmonicity (GHz)	-0.298594	0.046907	-0.346217	-0.307314	-0.305897	-0.304007	0.0
Readout assignment error	0.044305	0.062403	0.002900	0.011950	0.025300	0.044150	0.490000
Prob. measure $ 0\rangle$ prepare $ 1\rangle$	0.044364	0.056621	0.004400	0.013800	0.025600	0.046700	0.312400
Prob. measure $ 1\rangle$ prepare $ 0\rangle$	0.044246	0.074209	0.001400	0.010200	0.023600	0.044400	0.667600
Readout length (ns)	4000	0.0	4000	4000	4000	4000	4000
ID error	0.001259	0.005361	0.000141	0.000256	0.000360	0.000569	0.048093
The Z-axis rotation (R_Z) error	0.0	0.0	0.0	0.0	0.0	0.0	0.0
The \sqrt{X} (SX) error	0.001259	0.005361	0.000141	0.000256	0.000360	0.000569	0.048093
Pauli-X error	0.001259	0.005361	0.000141	0.000256	0.000360	0.000569	0.048093

TABLE XV: Summary of hardware performance, qubit characteristics, and key specifications for the 127-qubit quantum computer *ibm_strasbourg*. The basis gates of this machine are ECR, RZ, SX, ID, X. The processor type is *Eagle r3* (version 1.10.11). As of July 3, 2024, the system demonstrates a median ECR error of 8.857×10^{-3} , and a median gate time of 660 ns.

System parameters	Mean	StDev	Min	1 st Quartile	Median	3 rd Quartile	Max
T1 (μ s)	292.823565	119.937196	40.243743	200.07130	287.181909	364.642999	707.960349
T2 (μ s)	199.708814	128.709167	12.680931	87.916392	187.396030	290.491071	510.203219
Frequency (GHz)	4.815512	0.120955	4.536352	4.729195	4.816615	4.900868	5.107659
Anharmonicity (GHz)	-0.263911	0.107956	-0.319817	-0.309432	-0.308260	-0.305938	0.0
Readout assignment error	0.034652	0.044990	0.003600	0.010100	0.017100	0.041000	0.346300
Prob. measure $ 0\rangle$ prepare $ 1\rangle$	0.033777	0.052202	0.003600	0.009600	0.016200	0.037000	0.344800
Prob. measure $ 1\rangle$ prepare $ 0\rangle$	0.035527	0.049744	0.002400	0.009800	0.015800	0.035400	0.347800
Readout length (ns)	1600	0.0	1600	1600	1600	1600	1600
ID error	0.001408	0.008712	0.000084	0.000183	0.000244	0.000454	0.095269
The Z-axis rotation (R_Z) error	0.0	0.0	0.0	0.0	0.0	0.0	0.0
The \sqrt{X} (SX) error	0.001408	0.008712	0.000084	0.000183	0.000244	0.000454	0.095269
Pauli-X error	0.001408	0.008712	0.000084	0.000183	0.000244	0.000454	0.095269

TABLE XVI: Summary of hardware performance, qubit characteristics, and key specifications for the 127-qubit quantum computer *ibm-osaka*. The basis gates employed by this system include ECR, RZ, SX, ID, and X. The processor type is *Eagle r3* (version 1.1.8). As of July 3, 2024, the system demonstrates a median ECR error of 8.596×10^{-3} , and a median gate time of 660 ns.

System parameters	Mean	StDev	Min	1 st Quartile	Median	3 rd Quartile	Max
T1 (μ s)	275.209175	93.340756	7.717160	222.16072	278.368365	335.722431	440.616889
T2 (μ s)	144.771406	99.247376	8.117184	60.099590	132.372260	213.681193	409.977824
Frequency (GHz)	4.854223	0.114444	4.568035	4.772079	4.861266	4.928279	5.128348
Anharmonicity (GHz)	-0.284977	0.079198	-0.311990	-0.308883	-0.307491	-0.306113	0.0
Readout assignment error	0.051915	0.076861	0.003500	0.011500	0.021900	0.060600	0.493100
Prob. measure $ 0\rangle$ prepare $ 1\rangle$	0.053071	0.082672	0.003600	0.011000	0.022600	0.058500	0.500000
Prob. measure $ 1\rangle$ prepare $ 0\rangle$	0.050758	0.085043	0.002000	0.010100	0.021000	0.062600	0.689600
Readout length (ns)	1400	0.0	1400	1400	1400	1400	1400
ID error	0.001470	0.006991	0.000077	0.000170	0.000250	0.000432	0.062575
The Z-axis rotation (R_Z) error	0.0	0.0	0.0	0.0	0.0	0.0	0.0
The \sqrt{X} (SX) error	0.001470	0.006991	0.000077	0.000170	0.000250	0.000432	0.062575
Pauli-X error	0.001470	0.006991	0.000077	0.000170	0.000250	0.000432	0.062575

TABLE XVII: Summary of hardware performance, qubit characteristics, and key specifications for the 127-qubit quantum computer *ibm-cleveland*. The basis gates of this machine are ECR, RZ, SX, ID, X. The processor type is *Eagle r3* (version 1.5.1). As of July 3, 2024, the system demonstrates a median ECR error of 9.157×10^{-3} , and a median gate time of 590.222 ns.

System parameters	Mean	StDev	Min	1 st Quartile	Median	3 rd Quartile	Max
T1 (μ s)	211.979707	72.812847	18.787932	172.508265	213.579840	256.393505	454.759059
T2 (μ s)	196.083432	119.767324	14.467346	102.122094	191.647308	274.766102	523.275907
Frequency (GHz)	4.876390	0.123974	4.589666	4.795009	4.876078	4.948031	5.238570
Anharmonicity (GHz)	-0.308475	0.004577	-0.324563	-0.310648	-0.308918	-0.307588	-0.278350
Readout assignment error	0.029770	0.047776	0.004500	0.009250	0.013000	0.024600	0.323700
Prob. measure $ 0\rangle$ prepare $ 1\rangle$	0.026925	0.035570	0.004600	0.011100	0.014800	0.024900	0.256400
Prob. measure $ 1\rangle$ prepare $ 0\rangle$	0.032615	0.065273	0.003200	0.006400	0.010600	0.022000	0.391000
Readout length (ns)	1251.556	0.0	1251.556	1251.556	1251.556	1251.556	1251.556
ID error	0.000445	0.000847	0.000100	0.000202	0.000278	0.000401	0.009188
The Z-axis rotation (R_Z) error	0.0	0.0	0.0	0.0	0.0	0.0	0.0
The \sqrt{X} (SX) error	0.000445	0.000847	0.000100	0.000202	0.000278	0.000401	0.009188
Pauli-X error	0.000445	0.000847	0.000100	0.000202	0.000278	0.000401	0.009188

TABLE XVIII: Summary of hardware performance, qubit characteristics, and key specifications for the 127-qubit quantum computer *ibm-cusco*. The basis gates employed by this system include ECR, RZ, SX, ID, and X. The processor type is *Eagle r3* (version 1.0.40). As of July 3, 2024, the system demonstrates a median ECR error of 2.398×10^{-2} , and a median gate time of 460 ns.

System parameters	Mean	StDev	Min	1 st Quartile	Median	3 rd Quartile	Max
T1 (μ s)	136.288638	63.328683	26.825990	80.328785	135.758247	184.787286	346.403520
T2 (μ s)	96.987691	71.929940	2.803230	47.662439	72.346176	142.604449	346.467411
Frequency (GHz)	5.164246	0.133437	4.806652	5.071311	5.168677	5.263250	5.462529
Anharmonicity (GHz)	-0.299714	0.038185	-0.322850	-0.305927	-0.304439	-0.302885	0.0
Readout assignment error	0.060970	0.073258	0.005000	0.019450	0.038100	0.065900	0.392800
Prob. measure $ 0\rangle$ prepare $ 1\rangle$	0.072222	0.087468	0.007800	0.018400	0.039000	0.085767	0.429000
Prob. measure $ 1\rangle$ prepare $ 0\rangle$	0.049717	0.072154	0.0	0.014300	0.026000	0.049833	0.377600
Readout length (ns)	4000	0.0	4000	4000	4000	4000	4000
ID error	0.002483	0.006949	0.000138	0.000262	0.000565	0.001776	0.058174
The Z-axis rotation (R_Z) error	0.0	0.0	0.0	0.0	0.0	0.0	0.0
The \sqrt{X} (SX) error	0.002483	0.006949	0.000138	0.000262	0.000565	0.001776	0.058174
Pauli-X error	0.002483	0.006949	0.000138	0.000262	0.000565	0.001776	0.058174

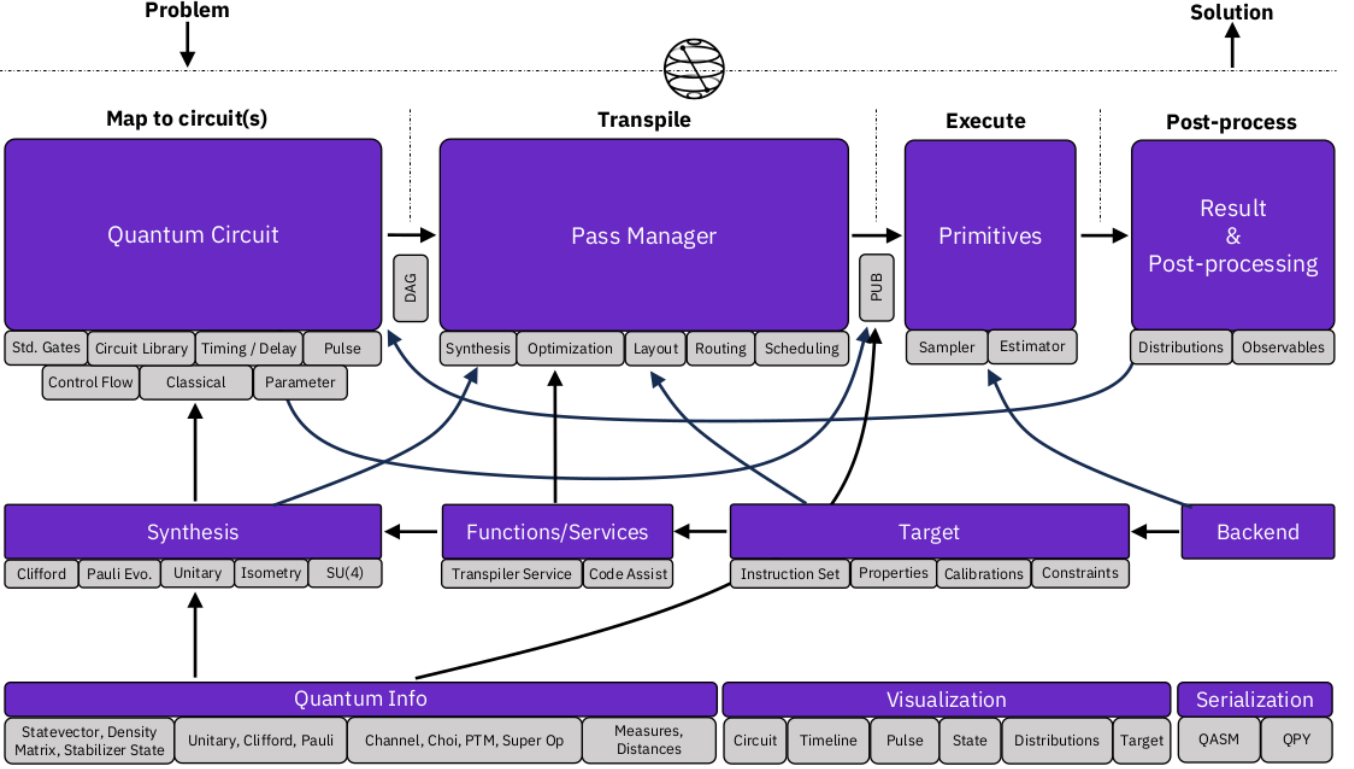


FIG. 5: Qiskit’s software architecture: The quantum info module links circuits to quantum information mathematics. The transpiler optimizes circuits via a pass manager, considering ISA and constraints. Primitives run circuits on simulators or hardware, evaluating results. Visualization tools and serialization with OpenQASM [70] and QPY format are also included [71]. Regenerated under a Creative Commons license (<https://creativecommons.org/licenses/by/4.0/>) from [46].

- *Mapping the Problem.* Begin by constructing a function that generates a **QuantumCircuit** specifically designed to prepare an n-qubit GHZ state. Then, apply this function to generate a 100-qubit GHZ state and collect the relevant observables for measurement.

```
# Step 1: Mapping the problem
from qiskit import QuantumCircuit

def create_n_qubit_GHZ_circuit(n_qubits: int) -> QuantumCircuit:
    """Generates a QuantumCircuit for an n_qubit GHZ state.

    Args:
        n_qubits (int): Number of qubits in the n-qubit GHZ
        -> state

    Returns:
        QuantumCircuit: Quantum circuit that prepares the
        -> n-qubit GHZ state
    """
    if isinstance(n_qubits, int) and n_qubits >= 2:
        ghz_circuit = QuantumCircuit(n_qubits)
        ghz_circuit.h(0)
        for i in range(n_qubits-1):
            ghz_circuit.cx(i, i+1)
    else:
        raise ValueError("Invalid input: n_qubits must be >= 2")

    return ghz_circuit

# creating a 100-qubit GHZ state
n_qubits = 100
ghz_circuit = create_n_qubit_GHZ_circuit(n_qubits)
```

Next, proceed to map to the operators of interest. In

this case, the focus is on ZZ operators between qubits to analyze their behavior over increasing distances. The goal is to observe how expectation values become progressively less accurate (more corrupted), indicating the extent of noise present in the system.

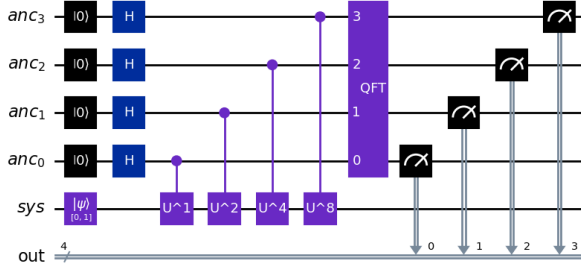
```
# Next, mapping to relevant operators
from qiskit.quantum_info import SparsePauliOp

# Create a list of operator strings for ZZ terms
operator_strings = ['Z' + 'I'*i + 'Z' + 'I'*(n_qubits-2-i) for i
-> in range(n_qubits-1)]
print(operator_strings)
print(len(operator_strings))

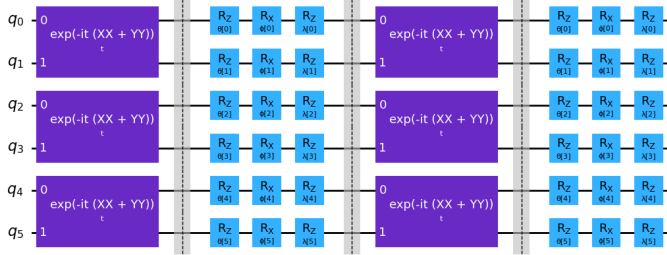
# Create SparsePauliOp objects for each operator string
operators = [SparsePauliOp(operator) for operator in
-> operator_strings]
```

- *Optimization for quantum hardware execution.* Optimize the problem to align with the Instruction Set Architecture (ISA) of the backend.

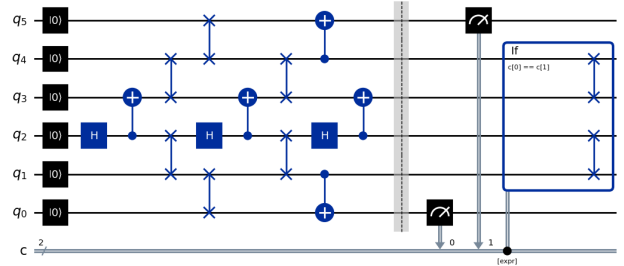
a) High-level abstract circuit composition
(example: quantum phase estimation)



c) Parameterized circuits
(example: twirled Trotterized evolution)



b) Standard gates and classical control flow
(example: entanglement distillation)



d) Hardware native gates and timing (ISA circuit)
(example: GHZ with dynamical decoupling)

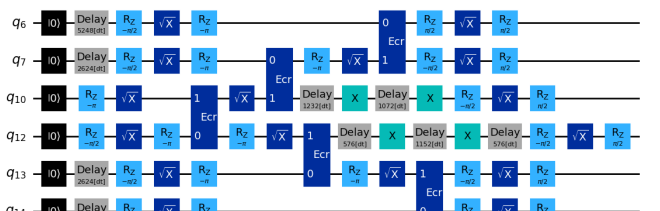


FIG. 6: Examples of Qiskit circuits: (a) Quantum phase estimation algorithm [72]. (b) Entanglement distillation circuit with fallback logic for Bell state preparation [73]. (c) Trotterized $XX + YY$ Hamiltonian simulation circuit [74] with Pauli twirling for noise suppression [75]. (d) GHZ state preparation circuit optimized for hardware ISA, using dynamical decoupling to reduce noise [76]. Regenerated under a Creative Commons license (<https://creativecommons.org/licenses/by/4.0/>) from [46].

```
# Step 2: Optimization for quantum hardware execution
from qiskit.transpiler.preset_passmanagers import
    generate_preset_pass_manager
from qiskit_ibm_runtime import QiskitRuntimeService

# Instantiate QiskitRuntimeService
service = QiskitRuntimeService()

# Find the least busy backend with at least 100 qubits
backend = service.least_busy(simulator=False, operational=True,
    min_num_qubits=100)

# Generate a preset pass manager for optimization
pm = generate_preset_pass_manager(optimization_level=1,
    backend=backend)

# Run the pass manager on the initial state preparation circuit
optimized_circuit = pm.run(ghz_circuit)

# Apply layout to operators
isa_operators_list = [op.apply_layout(optimized_circuit.layout)
    for op in operators]
```

```
# Step 3: Execution on quantum hardware
from qiskit_ibm_runtime import EstimatorOptions
from qiskit_ibm_runtime import EstimatorV2 as Estimator

# Define options for the Estimator
options = EstimatorOptions()
options.resilience_level = 1
options.optimization_level = 0
options.dynamical_decoupling.enable = True
options.dynamical_decoupling.sequence_type = "XY4"

# Create an Estimator object
estimator = Estimator(backend, options=options)

# Submit the circuit and operators list to the Estimator
job = estimator.run([(optimized_circuit, isa_operators_list)])
job_id = job.job_id()
print(job_id)
```

- *Execution on quantum hardware.* Proceed to submit the job for execution on the quantum hardware, implement error suppression using a technique known as dynamical decoupling to mitigate errors, and adjust the resilience level to determine the degree of error resilience desired. Higher resilience levels yield more precise results but require longer processing times.

- *Post-processing of results.* Visualize the results through plotting after the job execution is finished. Observing the expectation value $\langle Z_0 Z_i \rangle$ decreases as i increases, indicating a deviation from the ideal scenario where all $\langle Z_0 Z_i \rangle$ values should ideally be 1 in simulation.

```

# Step 4: Post-processing of results

import matplotlib.pyplot as plt
import numpy as np
from qiskit_ibm_runtime import QiskitRuntimeService

# Define data: Distance between the Z operators
data = list(range(1, len(operators) + 1))

# Retrieve results from the job
result = job.result()[0]

# Extract expectation values from the result
values = result.data.evs

# Normalize the expectation values relative to the first value
values = [v / values[0] for v in values]

# Plotting the graph
plt.scatter(data, values, marker='o', label='100-qubit GHZ
→ state')
plt.xlabel('Distance between qubits $i$')
plt.ylabel(r'$\langle Z_0 Z_i \rangle / \langle Z_0 Z_1 \rangle$')
plt.legend()
plt.show()

```

For the 100-qubit GHZ state, the normalized expectation value $\langle Z_0 Z_i \rangle / \langle Z_0 Z_1 \rangle$ is crucial for understanding the quantum correlations among the qubits. Figure 7 illustrates how the signal decays with increasing distance between qubits, reflecting the presence of noise in the system. To delve deeper into quantum computing with Qiskit, we refer to the recent review in [46].

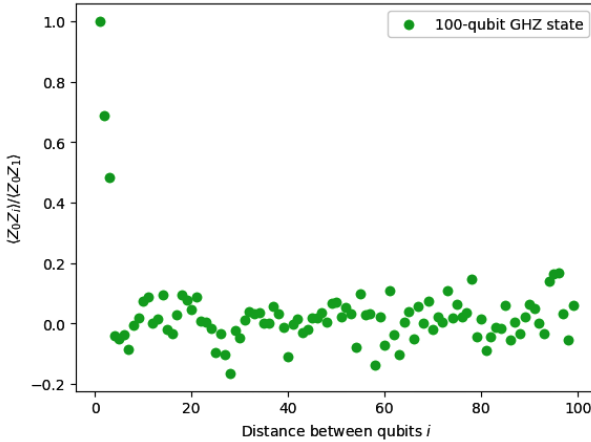


FIG. 7: Decay of normalized $\langle Z_0 Z_i \rangle / \langle Z_0 Z_1 \rangle$ expectation values for a 100-qubit GHZ state, demonstrating quantum correlations as distance between qubits increases. Reproduced from [69].

VI. TOWARD USEFUL QUANTUM COMPUTING

A. The IBM's era of quantum utility

In 2023, an IBM and UC Berkeley groundbreaking experiment revealed a path toward practical quantum computing [27, 77]. This experiment demonstrated that quantum computers could execute circuits beyond the capabilities of brute-force classical simulations. For the

first time, IBM Quantum has hardware and software capable of running quantum circuits at a scale of 100 qubits and 3,000 gates without prior knowledge of the outcomes [28, 35].

These advancements have prompted IBM Quantum to advocate moving beyond traditional circuit models by embracing parallelism, concurrent classical computing, and dynamic circuits. IBM Quantum emphasizes the necessity of a heterogeneous computing architecture that integrates scalable, parallel circuit execution with advanced classical computation [28, 35].

IBM Quantum's vision for the future involves quantum-centric supercomputing [66, 67]. At the IBM Quantum Summit 2023, significant updates were announced, bringing us closer to this goal, alongside an extended roadmap outlining IBM Quantum's journey toward quantum-centric supercomputing over the next decade. This will enable more advanced utility-scale work and provide a seamless development environment for IBM Quantum's users, potentially even before achieving fault tolerance [27, 28, 33, 35, 78, 79].

B. IBM Quantum's roadmap

To guide IBM Quantum's mission towards achieving quantum-centric supercomputing, IBM Quantum is extending its roadmap to 2033, spanning a decade of quantum innovation. The roadmap emphasizes advancements in the number of gates that IBM Quantum's processors and systems can execute. Beginning with *Heron* targeting 5,000 gates by 2024, successive generations of processors will leverage improvements in quality to achieve increasingly higher gate counts [35].

In 2029, a pivotal milestone: the *Starling* processor is projected to execute 100 million gates across 200 qubits, incorporating error correction based on the innovative Gross code. This code, represents an important advancement in error correction for near-term quantum computers [33, 80].

Following this, *Blue Jay* is envisioned as a system capable of executing 1 billion gates across 2,000 qubits by 2033. This milestone signifies a nine-order-of-magnitude increase in gate execution capability since IBM Quantum first introduced its cloud-based devices in 2016 [35].

The innovation roadmap will demonstrate the necessary technology to implement the Gross code through processors named *Flamingo*, *Crossbill*, and *Kookaburra*, utilizing l-, m-, and c-couplers, respectively [33, 80].

C. IBM Quantum safe

Advancements in quantum technology highlight the need for new cryptographic methods based on mathematical challenges that are challenging for both quantum and classical computers to solve. IBM Quantum Safe

Quantum roadmap

The future of computing is quantum-centric.

Updated May 2024
✓ completed
⌚ pushed to next year
⌚ on target

Quantum journey	2023	2024	2025	2027	2029	2030+
Strategy overview	✓ Introduce parallelization of quantum computations.	⌚ Expand the utility of quantum computing.	✓ Demonstrate quantum-centric supercomputing.	✓ Scale quantum computing.	✓ Deliver a fully error-corrected system.	✓ Deliver quantum-centric supercomputers with 2,000's of logical qubits.
Why this matters to our clients and the world	✓ Today, our systems are capacity limited and user jobs can take multiple days. Efficient parallelization between QPUs and parallelization of quantum and classical resources will enable efficient near-term algorithms.	⌚ Qiskit Primitives with error mitigation will provide the foundation platform where algorithm and application developers can focus on the workflow and get the best quality out of the quantum hardware.	In 2025, we will enhance the quality of quantum circuits to allow running 7,500 gates and bring together modular processors, middleware, and quantum communication to demonstrate the first quantum-centric supercomputer.	We will scale qubits, electronics, infrastructure, and software to reduce footprint, cost, and energy usage. The quality of quantum circuits will improve to allow running 10,000 gates.	We will bring users a quantum system with 200 qubits capable of running 100 million gates.	Beyond 2033, quantum-centric supercomputers will include thousands of qubits capable of running 1 billion gates, unlocking the full power of quantum computing.
The technology or innovations that will make this possible	✓ Middleware will automatically distribute tasks. Serverless tools will allow users to focus on code and not the infrastructure. ⌚ Expanded classical resources in Qiskit Runtime will speed up compilation and maximize the utilization of the QPUs.	⌚ Built-in error mitigation will automatically determine the best method to reduce the effect of noise. ⌚ Transpiler services will optimally rewrite circuits for hardware, taking advantage of AI. Watson Code Assistant will help users write Qiskit code to program quantum systems.	A quantum node will be part of a network incorporating classical and quantum communication. Resource management will handle quantum and classical workflows. Qiskit will provide libraries of quantum functions and higher-level APIs for faster algorithm and application development.	Intelligent orchestration will analyze workflows to identify the optimal resource allocation (QPUs, communication, and classical resources) for the task. Qiskit will orchestrate approaches to handle errors to provide noise-free outputs to the users.	Users will be able to run large-scale problems using high-rate quantum error correction.	Quantum computers running algorithms using thousands of logical qubits are expected to enable general applications in security, chemistry, machine learning, and optimization.
How these advancements will be delivered to IBM clients and partners	✓ Multiple 100+ qubit Eagle processors will be connected using classical communication. Ahead-of-time compilation will increase utilization of the QPUs.	⌚ Multiple higher-quality 100+ qubit Heron processors will be connected using classical communication.	Pre-built Qiskit functions and optimized libraries will be available. A 1,000+ qubit Flamingo system will be demonstrated, made from multiple processors, with each processor made from multiple chips.	The performance of our Flamingo systems will improve to allow users to run circuits with up to 10,000 gates and 1,000+ qubits.	The Starling system will be available to clients. It will be a modular, error-corrected quantum-centric supercomputer with 200 qubits capable of running a total of 100 million gates.	Our 100,000-qubit Blue Jay system will define 2,000 qubits capable of running a total of 1 billion gates. The middleware will integrate this system into ever more powerful quantum-centric supercomputers.

FIG. 8: IBM Quantum's technology roadmap, starting with the introduction of parallelization of quantum computation in 2023, aiming to expand the utility of quantum computing in 2024, and advancing to the delivery of quantum-centric supercomputers with thousands of logical qubits in 2030 and beyond. Accessible at [81].

aids enterprises in evaluating their cryptographic security and updating their cybersecurity strategies for the era of practical quantum computing.

IBM Quantum Safe roadmap outlines ongoing efforts to advance research in quantum-safe cryptography, collaborate with industry partners to promote adoption of post-quantum cryptographic solutions, and innovate new quantum-safe technologies. This includes “IBM Quantum Safe Explorer,” a cryptographic discovery tool launched in October 2023 [82, 83].

Figure 8 illustrates IBM’s roadmap for quantum computing technology [81]. For detailed information on IBM Quantum’s previous and updated development roadmaps, their accomplishments in hardware, software, execution, orchestration, and their innovation roadmap, we refer readers to [80].

VII. CONCLUSION

This study illuminates the rapid evolution and promising future of quantum computing within IBM Quantum. From pioneering quantum hardware advancements to robust software frameworks like Qiskit, IBM continues to redefine the boundaries of quantum technology.

We have delved into IBM Quantum’s dynamic journey in quantum computing, providing comprehensive performance evaluations of current and retired quantum computers that illustrate their evolution and future prospects. The documented metrics underscore IBM Quantum’s unwavering commitment to advancing quantum computing technology, offering a comparative framework across different systems and highlighting significant technological strides over time.

As we move towards quantum-centric supercomputing and quantum-safe cryptography, IBM Quantum’s trajectory promises transformative capabilities. With ongoing innovations and collaborative efforts, IBM Quantum is poised to ushering in a new era of computing prowess, offering profound implications across scientific, industrial, and cryptographic domains.

Looking ahead, the evolution of quantum computing will require addressing remaining challenges and exploring new avenues for innovation and application. Collaborative efforts within the quantum computing community, including partnerships and open-source initiatives, will be pivotal in unlocking the full potential of quantum technologies. Moreover, substantial funding and investments at national and international levels will be crucial in driving research, development, and deployment of quantum technologies.

ACKNOWLEDGMENTS

I am deeply grateful to the crowns of honor, though words cannot fully express my appreciation. The views and conclusions presented in this work reflect the author’s perspective and do not necessarily align with those of IBM Quantum.

Funding

The author declares that no funding, grants, or other forms of support were received at any point throughout this research.

-
- [1] M. AbuGhanem and H. Eleuch, “NISQ computers: a path to quantum supremacy,” *IEEE Access*, **12**, 102941–102961 (2024).
 - [2] P. Dirac, “The principles of quantum mechanics,” Oxford, Clarendon Press, (1930).
 - [3] M. AbuGhanem, “Properties of some quantum computing models,” Master’s Thesis, Fac. Sci., Ain Shams Univ. (2019).
 - [4] D. R. Simon, “On the power of quantum computation,” *SIAM J. Comput.* **26**(5), 1474–1483 (1997).
 - [5] A. W. Harrow, A. Montanaro, “Quantum computational supremacy,” *Nature* **549**(7671), 203–209 (2017).
 - [6] M. AbuGhanem, “Information processing at the speed of light.” Elsevier, *SSRN* 4748781 (2024). <http://dx.doi.org/10.2139/ssrn.4748781>
 - [7] M. AbuGhanem, “Photonic Quantum Computers,” arXiv preprint arXiv:2409.08229, (2024).
 - [8] J. Preskill, “Quantum computing and the entanglement frontier,” *arXiv preprint arXiv:1203.5813v3* (2012).
 - [9] J. Preskill, “Quantum Computing in the NISQ era and beyond,” *Quantum* **2**, 79 (2018).
 - [10] IBM Research. “IBM Makes Quantum Computing Available on IBM Cloud to Accelerate Innovation.” May 2016. <https://www.prnewswire.com/news-releases/ibm-makes-quantum-computing-available-on-ibm-cloud-to-accelerate-innovation-300262512.html>. Retrieved July 29 (2024).
 - [11] W. J. Zeng. “Unsupervised Machine Learning on Rigetti 19Q with Forest 1.2.” Dec. 18, 2017. <https://medium.com/rigetti/unsupervised-machine-learning-on-rigetti-19q-with-forest-1-2-39021339699>. Retrieved July 29 (2024).
 - [12] Amazon. “AWS Announces General Availability of Amazon Braket.” August 13, 2020. <https://press.aboutamazon.com/2020/8/aws-announces-general-availability-of-amazon-braket>. Retrieved July 29 (2024).
 - [13] J. Russel. “Honeywell Debuts Quantum System, ‘Subscription’ Business Model, and Glimpse of Roadmap.” Oct. 2020. <https://www.hpcwire.com/2020/10/29/honeywell-debuts-new-quantum-system-and-subscription-business-model/>. Retrieved July 29 (2024).
 - [14] Google Quantum AI. “Google Quantum Computing Service.” <https://quantumai.google/cirq/google/conce>

- pts. Accessed July 29 (2024).
- [15] M. AbuGhanem, Google Quantum AI's Quest for Error-Corrected Quantum Computers. (2024).
- [16] Xanadu AI. "Xanadu launches photonic quantum cloud platform." September 2 (2020). <https://www.xanadu.ai/press/XANADU-LAUNCHES-PHOTONIC-QUANTUM-CLOUD-PLATFORM>. Retrieved July 29 (2024).
- [17] Oxford Quantum Circuits. <https://oqc.tech/>. Accessed July 29 (2024).
- [18] H. Silverio. "PASQAL - First Neutral Atoms Quantum Computer available on the cloud." May 6 (2022). <https://www.pasqal.com/news/pasqal-first-neutral-atoms-quantum-computer-available-on-the-cloud/>. Retrieved July 29 (2024).
- [19] QuEra. "QuEra's Quantum Computer 'Aquila' Now Available on Amazon Braket." November 1 (2022). <https://www.quera.com/press-releases/queras-quantum-computer-aquila-now-available-on-amazon-braket>. Retrieved July 29 (2024).
- [20] Quandela. "The first European quantum computer in the cloud, developed by Quandela." Nov. (2022). <https://www.quandela.com/wp-content/uploads/2022/11/Quandela-The-first-European-quantum-computer-on-the-cloud-developed-by-Quandela.pdf>. Accessed July 29 (2024).
- [21] K. Svore. "Azure Quantum is now in Public Preview." Feb. 2021. <https://cloudblogs.microsoft.com/quantum/2021/02/01/azure-quantum-preview/>. Retrieved July 29 (2024).
- [22] Strangeworks. "Strangeworks and IBM announce integration of IBM Quantum cloud services into the Strangeworks ecosystem." June 3, 2021. <https://strangeworks.com/press/strangeworks-and-ibm-announce-integration-of-ibm-quantum-cloud-services-into-the-strangeworks-ecosystem>. Retrieved July 29 (2024).
- [23] Deutsche Telekom. "T-Systems to offer quantum computing expertise and access to IBM Quantum computational resources." March 23, 2023. <https://www.telekom.com/en/media/media-information/archive/t-systems-launches-quantum-offering-1031464>. Retrieved July 29 (2024).
- [24] Elsevier. "Quantum computing research trends report." <https://www.elsevier.com/resources/quantum-computing-research-trends-report>. Accessed July 29 (2024).
- [25] T. L. Scholten *et al.* "Assessing the benefits and risks of quantum computers," *arXiv preprint arXiv:2401.16317v2* (2024).
- [26] IBM Quantum, <https://quantum.ibm.com/>, accessed August (2024).
- [27] Y. Kim *et al.* "Evidence for the utility of quantum computing before fault tolerance." *Nature* **618**, 500–505 (2023).
- [28] G. Wendum and J. Bylander, "Quantum computer scales up by mitigating errors," *Nature* **618**, 462–463 (2023).
- [29] U. Alvarez-Rodriguez *et al.* "Quantum Artificial Life in an IBM Quantum Computer," *Sci. Rep.* **8**, 14793 (2018).
- [30] IBM, "Exploring quantum use cases for chemicals and petroleum: Changing how chemicals are designed and petroleum is refined," <https://www.ibm.com/downloads/cas/BDGQRX0Z>, accessed (2023).
- [31] A. Kandala *et al.* "Hardware-efficient variational quantum eigensolver for small molecules and quantum magnets," *Nature*, September 13 (2017).
- [32] ExxonMobil, "ExxonMobil and IBM to Advance Energy Sector Application of Quantum Computing," (January 8, 2019). <https://news.exxonmobil.com/press-release/exxonmobil-and-ibm-advance-energy-sector-application-quantum-computing>, accessed (2023).
- [33] IBM Debuts Next-Generation Quantum Processor & IBM Quantum System Two, Extends Roadmap to Advance Era of Quantum Utility, December 4, 2023. <https://newsroom.ibm.com/2023-12-04-IBM-Debuts-Next-Generation-Quantum-Processor-IBM-Quantum-System-Two,-Extends-Roadmap-to-Advance-Era-of-Quantum-Utility>. Accessed July (2024).
- [34] O. Dial, "Eagle's quantum performance progress," 23 Mar 2022, <https://www.ibm.com/quantum/blog/eagle-quantum-processor-performance>
- [35] J. Gambetta, "The hardware and software for the era of quantum utility is here, We've entered a new era of quantum computing." December 4, 2023. <https://www.ibm.com/quantum/blog/quantum-roadmap-2023>, accessed July (2024).
- [36] D. Castelvecchi, IBM releases first-ever 1,000-qubit quantum chip, "The company announces its latest huge chip — but will now focus on developing smaller chips with a fresh approach to 'error correction?'" *Nature* **624**, 238 (2023).
- [37] P. Ball, "First quantum computer to pack 100 qubits enters crowded race," *Nature* **599**, 542 (2021).
- [38] J. Chow, O. Dial and J. Gambetta, "IBM Quantum breaks the 100-qubit processor barrier," 16 Nov. 2021 <https://www.ibm.com/quantum/blog/127-qubit-quantum-processor-eagle>, accessed (2024).
- [39] IBM Unveils 400 Qubit-Plus Quantum Processor and Next-Generation IBM Quantum System, *IBM Newsroom*, Nov 9, 2022, <https://newsroom.ibm.com/2022-11-09-IBM-Unveils-400-Qubit-Plus-Quantum-Processor-and-Next-Generation-IBM-Quantum-System-Two>, accessed (2023).
- [40] D. L. Underwood *et al.* "Using cryogenic CMOS control electronics to enable a two-qubit cross-resonance gate," *arXiv:2302.11538*, (2023).
- [41] Qiskit, <https://www.ibm.com/quantum/qiskit>, accessed (2024).
- [42] J. Chow *et al.* "Implementing a strand of a scalable fault-tolerant quantum computing fabric." *Nat Commun.* **5**, 4015 (2014).
- [43] Processor types, IBM Quantum documentation, <https://docs.quantum.ibm.com/guides/processor-types>, accessed July (2024).
- [44] S. Sheldon, E. Magesan and J. Chow, J. Gambetta, "Procedure for systematically tuning up cross-talk in the cross-resonance gate." *Phys. Rev. A* **93**, 060302(R). (2016).
- [45] Quantum processing units, IBM Quantum platform, <https://quantum.ibm.com/services/resources>, accessed July (2024).
- [46] A. Javadi-Abhari *et al.* "Quantum computing with Qiskit," *arXiv preprint arXiv:2405.08810* (2024).
- [47] The State of quantum open source software (2023): survey results. https://unitary.fund/posts/2023_survey_results.
- [48] R. S. Gupta *et al.* "Encoding a magic state with beyond break-even fidelity." *arXiv preprint arXiv:2305.13581* (2023).

- [49] M. AbuGhanem and H. Eleuch, “Two-qubit entangling gates for superconducting quantum computers,” *Results in Physics* **56**, 107236 (2024).
- [50] E. Bäumer *et al.* “Efficient Long-Range Entanglement using Dynamic Circuits.” *arXiv preprint arXiv:2308.13065* (2023).
- [51] R. C. Farrell *et al.* “Quantum Simulations of Hadron Dynamics in the Schwinger Model using 112 Qubits.” *arXiv preprint arXiv:2401.08044* (2024).
- [52] M. AbuGhanem *et al.* “Fast universal entangling gate for superconducting quantum computers,” *Elsevier, SSRN*, 4726035 (2024). <http://dx.doi.org/10.2139/ssrn.4726035>
- [53] E. H. Chen *et al.* “Realizing the Nishimori transition across the error threshold for constant-depth quantum circuits.” *arXiv preprint arXiv:2309.02863* (2023).
- [54] R. C. Farrell *et al.* “Scalable circuits for preparing ground states on digital quantum computers: The schwinger model vacuum on 100 qubits.” *PRX Quantum* **5**:020315 (2024).
- [55] R. Majumdar *et al.* “Best practices for quantum error mitigation with digital zero-noise extrapolation.” *arXiv preprint arXiv:2307.05203* (2023).
- [56] M. AbuGhanem, “Full quantum process tomography of a universal entangling gate on an IBM’s quantum computer,” *arXiv preprint arXiv:2402.06946* (2024).
- [57] J. A. Montanez-Barrera and K. Michielsen. “Towards a universal QAOA protocol: Evidence of quantum advantage in solving combinatorial optimization problems.” *arXiv preprint arXiv:2405.09169* (2024).
- [58] E. Pelofske *et al.* “Scaling Whole-Chip QAOA for Higher-Order Ising Spin Glass Models on Heavy-Hex Graphs.” *arXiv preprint arXiv:2312.00997* (2023).
- [59] M. AbuGhanem, “Comprehensive characterization of three-qubit Grover search algorithm on IBM’s 127-qubit superconducting quantum computers,” *arXiv preprint arXiv:2406.16018* (2024).
- [60] H. Yu *et al.* “Simulating large-size quantum spin chains on cloud-based superconducting quantum computers.” *Phys. Rev. Res.*, 5(1):013183 (2023).
- [61] T. Yasuda *et al.* “Quantum reservoir computing with repeated measurements on superconducting devices.” *arXiv preprint arXiv:2310.06706* (2023).
- [62] M. AbuGhanem and H. Eleuch, “Full quantum tomography study of Google’s Sycamore gate on IBM’s quantum computers,” *EPJ Quantum Technology* **11**(1), 36 (2024).
- [63] M. AbuGhanem and H. Eleuch, “Experimental characterization of Google’s Sycamore quantum AI on an IBM’s quantum computer,” *Elsevier, SSRN* 4299338 (2023). <http://dx.doi.org/10.2139/ssrn.4299338>.
- [64] V. Zhang and P. D. Nation. “Characterizing quantum processors using discrete time crystals.” *arXiv preprint arXiv:2301.07625* (2023).
- [65] M. Cerezo *et al.* “Variational quantum algorithms.” *Nature Reviews Physics*, **3**(9):625–644 (2021).
- [66] Y. Alexeev *et al.* “Quantum-centric supercomputing for materials science: A perspective on challenges and future directions.” *Future Generation Computer Systems*, (2024).
- [67] J. Robledo-Moreno *et al.* “Chemistry Beyond Exact Solutions on a Quantum-Centric Supercomputer.” *arXiv preprint arXiv:2405.05068* (2024).
- [68] I. Faro *et al.* “Middleware for quantum: An orchestration of hybrid quantum-classical systems.” *In 2023 IEEE International Conference on Quantum Software (QSW)* 1-8. IEEE (2023).
- [69] Scale to large number of qubits, IBM Quantum documentation, <https://docs.quantum.ibm.com/guides/hello-world#scale-to-large-numbers-of-qubits>, accessed July (2024).
- [70] A. Cross *et al.* “OpenQASM 3: A broader and deeper quantum assembly language.” *ACM Trans. Quan. Comp.*, 3(3):1–50 (2022).
- [71] D. Kremer *et al.* “Practical and efficient quantum circuit synthesis and transpiling with reinforcement learning.” *arXiv preprint arXiv:2405.13196* (2024).
- [72] A. Yu. Kitaev. “Quantum measurements and the Abelian stabilizer problem.” *arXiv preprint arXiv:quant-ph/9511026*, (1995).
- [73] C. H. Bennett, D. P. DiVincenzo, J. A. Smolin, and W. K. Wootters. “Mixed-state entanglement and quantum error correction.” *Phys. Rev. A*, **54**(5):3824 (1996).
- [74] S. Lloyd. “Universal quantum simulators.” *Science*, **273**(5278):1073–1078 (1996).
- [75] C. H. Bennett *et al.* “Purification of noisy entanglement and faithful teleportation via noisy channels.” *Phys. rev. lett.*, **76**(5):722 (1996).
- [76] L. Viola, E. Knill, and S. Lloyd. “Dynamical decoupling of open quantum systems.” *Phys. Rev. Lett.*, **82**(12):2417 (1999).
- [77] R. Mandelbaum, “A new paper from IBM and UC Berkeley shows a path toward useful quantum computing. A useful application for 127-qubit quantum processors with error mitigation.” June 14, 2023. <https://www.ibm.com/quantum/blog/utility-toward-useful-quantum>
- [78] Q. Xu *et al.* “Constant-Overhead Fault-Tolerant Quantum Computation with Reconfigurable Atom Arrays,” *arXiv preprint arXiv:2308.08648v1* (2023).
- [79] S. Bravyi *et al.* “High-threshold and low-overhead fault-tolerant quantum memory,” *Nature* **627**, 778–782 (2024).
- [80] Development & Innovation Roadmap, IBM Quantum, https://www.ibm.com/quantum/assets/IBM_Quantum_Development_&_Innovation_Roadmap.pdf, accessed August (2024).
- [81] IBM Quantum’s technology roadmap, <https://www.ibm.com/roadmaps/quantum.pdf>, Accessed August (2024).
- [82] Make the world quantum safe, <https://www.ibm.com/quantum/quantum-safe>, Accessed August 1st (2024).
- [83] IBM Quantum Safe Explorer: Simplify the discovery of cryptography and the management of quantum security risks, IBM Quantum, <https://www.ibm.com/downloads/cas/05B0WVZ>. Accessed August 1st (2024).

Appendix A: Characteristics of IBM's Quantum Computers

This section offers detailed performance summaries for various retired IBM Quantum's quantum computers, and some old performance data from current systems. Tables XIX to XLII provide key specifications such as coherence times (T1 and T2), qubit frequencies, gate error rates, qubit counts, basis gates, connections, and calibration dates, documented for historical and educational purposes within the literature of NISQ computing era. This enables a comparative assessment of different IBM Quantum systems, highlighting advancements in technology over time. These retired systems, alongside quantum simulators, have laid the groundwork for newer generations that continue to push the boundaries of quantum computing.

TABLE XIX: Hardware performance and qubit properties of the 433 qubit *ibm-seattle* quantum computer. The processor type is *Osprey* r1. The basis gates of this machine are: ECR, ID, RZ, SX, X. With a median ECR error: 2.155×10^{-2} , a median SX error: 6.256×10^{-4} , a median readout error: 4.910×10^{-2} , a median T1: $88.35 \mu\text{s}$, and a median T2: $58.73 \mu\text{s}$. Accessed June 29, 2023.

System characteristics	Min.	Mean	1 st Quartile	Median	3 rd Quartile	Stdev.	StdError	Max.	Unit
T1	1.318680	91.67790	66.47356	88.34887	110.75190	38.68508	1.901270	237.9175	μs
T2	4.769450	61.86490	33.40824	58.73242	84.342912	34.52344	1.696730	181.6891	μs
Frequency	0.0	4.967799	5.094863	5.181795	5.2812598	1.072827	0.051566	5.526796	GHz
Anharmonicity	-0.402713	-0.278956	-0.301865	-0.300014	-0.2974234	0.075007	0.003605	0.0	GHz
Readout assignment error	0.72	11.20224	1.970000	4.909999	10.93	20.31924	0.976480	100	$\times 10^{-2}$
Prob. meas 0⟩ prep 1⟩	0.40	7.066876	2.085	4.380	9.655	7.168634	0.352319	51.580	$\times 10^{-2}$
Prob. meas 1⟩ prep 0⟩	0.36	7.187085	1.72	4.18	9.635	8.260245	0.405969	71.64	$\times 10^{-2}$
Readout length	2000	2000	2000	2000	2000	0.0	0.0	2000	ns
ID error	0.179	45.722	0.4599	0.625	1.290	204.837	9.843	1000	$\times 10^{-3}$
\sqrt{X} (SX) error	0.179	45.722	0.4599	0.625	1.290	204.837	9.843	1000	$\times 10^{-3}$
Pauli-X error	0.179	45.722	0.4599	0.625	1.290	204.837	9.843	1000	$\times 10^{-3}$
ECR Error	7.198471	109.2662	15.51089	21.54787	39.877844	264.56291	11.78457	1000	$\times 10^{-3}$
ECR Gate time	135	635	660	660	660	138.9054	6.187339	1404	ns

TABLE XX: Summary of hardware performance, qubit characteristics and key specifications for the 127-qubits quantum computer *ibm-sherbrooke*, featuring basis gates ECR, ID, RZ, SX, and X. The processor type is *Eagle* r3, and calibration data was accessed on June 30, 2023.

System characteristics	Min.	Mean	1 st Quartile	Median	3 rd Quartile	Stdev.	StdError	Max.	Unit
T1	18.19069	281.5453	212.7437	289.0375	352.64895	104.2918	9.254408	513.9483	μs
T2	1.973268	180.1907	83.12792	168.4437	258.97337	106.4481	9.445748	392.8104	μs
Frequency	4.455260	4.790289	4.731587	4.794001	4.8593516	0.109099	0.009681	5.057533	GHz
Anharmonicity	-0.32426	-0.31039	-0.31225	-0.31093	-0.309626	0.005480	0.000486	-0.27186	GHz
Readout assignment error	0.0023	1.990682	0.649999	1.0	1.98	3.338019	0.296201	27.67	$\times 10^{-2}$
Prob. meas 0⟩ prep 1⟩	0.0020	2.141312	0.750	1.14	2.17	4.084455	0.362436	41.44	$\times 10^{-2}$
Prob. meas 1⟩ prep 0⟩	0.0012	1.870131	0.460	0.82	1.95	3.596563	0.319143	32.86	$\times 10^{-2}$
Readout length	1244.444	1244.444	1244.444	1244.444	1244.444	0.0	0.0	1244.444	ns
ID error	0.552649	5.274019	1.678334	2.149589	3.233953	11.90043	1.055992	111.4219	$\times 10^{-4}$
\sqrt{X} (SX) error	0.552649	5.274019	1.678334	2.149589	3.233953	11.90043	1.055992	111.4219	$\times 10^{-4}$
Pauli-X error	0.552649	5.274019	1.678334	2.149589	3.233953	11.90043	1.055992	111.4219	$\times 10^{-4}$
ECR Error	2.771444	45.41823	5.559371	7.494834	11.50235	182.0391	15.11699	1000	$\times 10^{-3}$
ECR Gate time	448	538.4691	533.3334	533.3334	533.3334	40.83243	3.402702	881.7778	ns

TABLE XXI: Summary of hardware performance, qubit characteristics and key specifications for the 127-qubits quantum computer *ibm_washington*, featuring basis gates CX, ID, IF_ELSE, RZ, SX and X. The processor type is *Eagle r3*. The system boasts 288 CX qubit connections, and calibration data was accessed on November 12, 2022.

System characteristics	Min.	Mean	1 st Quartile	Median	3 rd Quartile	Stdev.	StdError	Max.	Unit
T1	30.33	99.99779	84.46	99.68	116.815	27.40558	2.43185	188.64	μs
T2	5.33	96.948	60.7	94.13	135.75	49.201	4.3658	245.74	μs
Frequency	4.766	5.064	4.985	5.017	5.1405	0.1132	0.01	5.292	GHz
Anharmonicity	-0.3249	-0.30671	-0.3086	-0.3074	-0.3056	0.0053	0.0005	-0.27711	GHz
Readout assignment error	0.180	3.000	0.54	1.25	3.27	5.25	0.47	38.39	×10 ⁻²
Prob. meas 0⟩ prep 1⟩	0.22	3.17	0.73	0.14	2.91	5.34	0.47	39.56	×10 ⁻²
Prob. meas 1⟩ prep 0⟩	0.00	2.831	0.16	0.9	3.67	5.36579	0.4761365	37.22	×10 ⁻²
Readout length	864	864	864	864	864	0.0	0.0	864	ns
Single-qubit error	1.720	8.636	2.2	3.0	4.8	22.3	2.0	210.6	×10 ⁻⁴
CX Error	5.542	38.352	9.05025	12.31	18.2325	141.941	8.3931	1,000	×10 ⁻³
Gate time	270.222	567.621	405.333	469.333	689.778	224.770	13.314	1187.556	ns

TABLE XXII: Summary of hardware performance, qubit characteristics and key specifications for the 127-qubit quantum computer *ibm_kyiv*, featuring basis gates CX, ID, RZ, SX and X. The processor type is *Eagle r3*. The system boasts 288 CX qubit connections, and calibration data was accessed on November 14, 2022.^a

System characteristics	Min.	Mean	1 st Quartile	Median	3 rd Quartile	Stdev.	StdError	Max.	Unit
T1	44.81	299.737	233.6	302.51	367.63	101.11256	8.9723	495.91	μs
T2	13.72	160.919	63.37	122.66	223.88	118.695	10.5325	512.18	μs
Frequency	4.341	4.6202	4.539	4.613	4.7025	0.1125	0.0099	4.959	GHz
Anharmonicity	-0.36821	-0.14058	-0.31176	0	0	0.156603	0.013896	0	GHz
Readout assignment error	0.06	1.4262	0.25	0.66	1.475	2.0975	0.1861	12.67	×10 ⁻²
Prob. meas 0⟩ prep 1⟩	0.06	1.4924	0.32	0.66	1.43	2.318	0.206	13.34	×10 ⁻²
Prob. meas 1⟩ prep 0⟩	0.0	1.36	0.12	0.46	1.43	2.5257	0.22412	19.36	×10 ⁻²
Readout length	867.556	867.556	867.556	867.556	867.556	0.0	0.0	867.556	ns
Single-qubit error	0.775	4.391	1.419	2.102	3.9875	10.509	0.9325	110.5	×10 ⁻⁴
CX Error	1.0	1.0	1.0	1.0	1.0	0.0	0.0	1.0	
Gate time	611.556	636.445	611.556	636.4445	661.333	24.9318	1.469	661.333	ns

^a This system was upgraded, for the up-to-date specification see Table VI.

TABLE XXIII: Summary of hardware performance, qubit characteristics and key specifications for the 65-qubit quantum computer *ibm_ithaca*, featuring basis gates CX, ID, RZ, SX and X. The processor type is *Hummingbird r3*. The system boasts 144 CX qubit connections, and calibration data was accessed on November 14, 2022.

System characteristics	Min.	Mean	1 st Quartile	Median	3 rd Quartile	Stdev.	StdError	Max.	Unit
T1	40.3	174.392	138.31	176.95	203.13	55.1419	6.8395	359.67	μs
T2	18.45	181.374	112.77	172.63	250.73	97.732	12.122	388.69	μs
Frequency	4.542	4.738	4.657	4.732	4.814	0.0977	0.01212	4.931	GHz
Anharmonicity	-0.35381	-0.33370	-0.33511	-0.33359	-0.3316	0.00555	0.00069	-0.31597	GHz
Readout assignment error	0.54	2.4563	1.01	1.6	2.49	2.4638	0.30559	13.43	×10 ⁻²
Prob. meas 0⟩ prep 1⟩	0.92	3.10369	1.64	2.44	3.66	2.73169	0.33882	18.84	×10 ⁻²
Prob. meas 1⟩ prep 0⟩	0.04	1.8089	0.26	0.84	1.92	2.7354	0.3393	14.46	×10 ⁻²
Readout length	4924.444	4924.444	4924.444	4924.444	4924.444	0.0	0.0	4924.444	ns
Single-qubit error	1.28	4.508	1.935	2.619	3.505	11.849	1.469	97.72	×10 ⁻⁴
CX Error	5.189	26.145	7.19425	10.325	13.53	116.408	9.7006	1000	×10 ⁻³
Gate time	512	536.889	512	536.889	561.778	24.976	2.081	561.778	ns

TABLE XXIV: Summary of hardware performance, qubit characteristics and key specifications for the 27-qubit quantum computer *ibmq_kolkata*, featuring basis gates CX, ID, IF_ELSE, RZ, SX and X. The processor type is *Falcon r5.11*. The system boasts 56 CX qubit connections, and calibration data was accessed on November 14, 2022.

System characteristics	Min.	Mean	1 st Quartile	Median	3 rd Quartile	Stdev.	StdError	Max.	Unit
T1	12.78	116.237	98.63	113.5	142.365	33.779	6.5008	187.18	μs
T2	17.11	89.102	43.165	72.28	118.005	57.1635	11.0011	214.92	μs
Frequency	4.869	5.08234	5.0005	5.102	5.1845	0.11219	0.02159	5.268	GHz
Anharmonicity	-0.37341	-0.34455	-0.34554	-0.34345	-0.34158	0.006158	0.001185	-0.34002	GHz
Readout assignment error	0.53	2.0348	0.8	1.25	1.735	3.0326	0.5836	16.19	×10 ⁻²
Prob. meas 0⟩ prep 1⟩	0.62	2.1845	0.97	1.28	2	3.0407	0.5852	15.92	×10 ⁻²
Prob. meas 1⟩ prep 0⟩	0.26	1.885	0.69	1.14	1.6	3.0727	0.5914	16.46	×10 ⁻²
Readout length	675.556	675.556	675.556	675.556	675.556	0.0	0.0	675.556	ns
Single-qubit error	1.466	3.071	1.793	1.911	2.4345	3.875	0.7457	20.97	×10 ⁻⁴
CX Error	3.807	44.957	5.3405	6.852	9.34445	185.741	24.821	1000	×10 ⁻³
Gate time	195.556	426.256	320	398.222	490.667	162.254	21.682	1059.556	ns

TABLE XXV: Summary of hardware performance, qubit characteristics and key specifications for the 27-qubit quantum computer *ibmq_montreal*, featuring basis gates CX, ID, RZ, SX and X. The processor type is *Falcon r4*. The system boasts 56 CX qubit connections, and calibration data was accessed on November 14, 2022.

System characteristics	Min.	Mean	1 st Quartile	Median	3 rd Quartile	Stdev.	StdError	Max.	Unit
T1	3.73	108.8945	88.765	103.68	135.875	44.5739	8.5783	201.49	μs
T2	3.2	87.5989	45.46	71.84	119.88	54.8127	10.5487	228.86	μs
Frequency	4.835	4.9979	4.956	5	5.054	0.0729	0.0140	5.105	GHz
Anharmonicity	-0.41989	-0.33589	-0.33825	-0.33722	-0.324475	0.0189245	0.0036419	-0.30385	GHz
Readout assignment error	0.83	2.6389	1.285	1.62	2.94	2.4865	0.4785	11.26	×10 ⁻²
Prob. meas 0⟩ prep 1⟩	1.36	2.9489	2.06	2.22	3.23	1.7696	0.3406	9.78	×10 ⁻²
Prob. meas 1⟩ prep 0⟩	0.2	2.32889	0.53	0.82	1.7	3.91839	0.75409	17.36	×10 ⁻²
Readout length	5201.778	5201.778	5201.778	5201.778	5201.778	0.0	0.0	5201.778	ns
Single-qubit error	1.965	3.882	2.528	3.539	5.114	1.637	0.315	6.78	×10 ⁻⁴
CX Error	5.76	13.295	7.821	10.2165	17.13	8.009	1.07009	43.78	×10 ⁻³
Gate time	270.222	442.921	368.00025	405.333	490.667	145.024	19.379	1059.556	ns

TABLE XXVI: Summary of hardware performance, qubit characteristics and key specifications for the 27-qubit quantum computer *ibmq_mumbai*, featuring basis gates CX, ID, IF_ELSE, RZ, SX and X. The processor type is *Falcon r5.10*. The system boasts 56 CX qubit connections, and calibration data was accessed on November 14, 2022.

System characteristics	Min.	Mean	1 st Quartile	Median	3 rd Quartile	Stdev.	StdError	Max.	Unit
T1	31.87	121.619	85.08	119.22	148.485	46.956	9.0367	223.51	μs
T2	22.37	104.237	64.5	112.75	148.515	53.239	10.24586	202.74	μs
Frequency	4.666	4.8799	4.782	4.893	4.965	0.1164	0.0224	5.076	GHz
Anharmonicity	-0.39107	-0.33315	-0.33317	-0.33129	-0.329925	0.012249	0.002357	-0.31416	GHz
Readout assignment error	1.15	2.9548	1.55	1.92	3.49	2.38318	0.45864	11.05	×10 ⁻²
Prob. meas 0⟩ prep 1⟩	1.74	4.1319	2.35	2.74	4.22	3.1897	0.6139	15.58	×10 ⁻²
Prob. meas 1⟩ prep 0⟩	0.54	1.7778	0.78	1.0	1.66	2.2369	0.4305	11.48	×10 ⁻²
Readout length	3552	3552	3552	3552	3552	0.0	0.0	3552	ns
Single-qubit error	1.488	16.795	2.031	2.648	3.843	70.478	13.564	369.3	×10 ⁻⁴
CX Error	5.062	88.451	7.28325	9.154	14.4975	256.875	34.326	1000	×10 ⁻³
Gate time	248.889	495.746	368.00025	430.2225	584.889	210.626	28.146	1351.111	ns

TABLE XXVII: Summary of hardware performance, qubit characteristics and key specifications for the 27-qubit quantum computer *ibm_cairo*, featuring basis gates CX, ID, IF_ELSE, RZ, SX and X. The processor type is *Falcon r5.11*. The system boasts 56 CX qubit connections, and calibration data was accessed on November 14, 2022.

System characteristics	Min.	Mean	1 st Quartile	Median	3 rd Quartile	Stdev.	StdError	Max.	Unit
T1	41.26	104.934	76.245	94.74	117.4	45.447	8.7462	221.09	μs
T2	12.82	102.974	42.35	113.14	145.66	73.9239	14.2267	303.4	μs
Frequency	4.911	5.1289	5.045	5.133	5.2135	0.1129	0.0217	5.284	GHz
Anharmonicity	-0.34568	-0.34074	-0.342275	-0.34054	-0.33929	0.002262	0.000435	-0.33714	GHz
Readout assignment error	0.58	2.04223	0.835	1.25	1.755	3.14460	0.60518	17.01	×10 ⁻²
Prob. meas 0⟩ prep 1⟩	0.82	2.48741	1.08	1.46	1.94	4.81937	0.92749	26.38	×10 ⁻²
Prob. meas 1⟩ prep 0⟩	0.34	1.5970	0.61	0.88	1.55	1.8856	0.3629	7.64	×10 ⁻²
Readout length	732.444	732.444	732.444	732.444	732.444	0.0	0.0	732.444	ns
Single-qubit error	1.357	7.0541	1.965	2.512	4.263	16.298	3.1366	84.63	×10 ⁻⁴
CX Error	4.894	89.897	8.0925	10.705	19.3425	256.469	34.272	1000	×10 ⁻³
Gate time	160	352.889	255.111	316.444	415.999	163.919	21.905	970.667	ns

TABLE XXVIII: Summary of hardware performance, qubit characteristics and key specifications for the 27-qubit quantum computer *ibm_auckland*, featuring basis gates CX, ID, IF_ELSE, RZ, SX and X. The processor type is *Falcon r5.11*. The system boasts 56 CX qubit connections, and calibration data was accessed on November 14, 2022.

System characteristics	Min.	Mean	1 st Quartile	Median	3 rd Quartile	Stdev.	StdError	Max.	Unit
T1	7.85	147.03	109.66	163.14	195.335	64.8467	12.4797	263.52	μs
T2	16.27	132.9515	61.52	129.95	178.725	87.51967	16.84317	308.12	μs
Frequency	4.692	4.9573	4.879	4.97	5.0355	0.1245	0.0239	5.204	GHz
Anharmonicity	-0.35079	-0.34432	-0.34513	-0.34389	-0.342655	0.002391	0.000460	-0.34066	GHz
Readout assignment error	0.64	2.98778	0.73	0.92	1.26	6.62509	1.27499	31.28	×10 ⁻²
Prob. meas 0⟩ prep 1⟩	0.74	3.4312	0.91	0.96	1.44	10.506	2.0219	55.64	×10 ⁻²
Prob. meas 1⟩ prep 0⟩	0.4	2.54445	0.56	0.74	1.08	6.29405	1.21129	32.78	×10 ⁻²
Readout length	757.333	757.333	757.333	757.333	757.333	0.0	0.0	757.333	ns
Single-qubit error	1.533	44.774	1.8965	2.564	3.399	216.890	41.741	1130	×10 ⁻⁴
CX Error	4.257	117.431	5.704	8.9255	16.24	308.699	41.252	1000	×10 ⁻³
Gate time	135.111	479.746	353.778	432	560.00025	258.922	34.5999	1564.444	ns

TABLE XXIX: Summary of hardware performance, qubit characteristics and key specifications for the 27-qubit quantum computer *ibm_hanoi*, featuring basis gates CX, ID, IF_ELSE, RZ, SX and X. The processor type is *Falcon r5.11*. The system boasts 56 CX qubit connections, and calibration data was accessed on November 14, 2022.

System characteristics	Min.	Mean	1 st Quartile	Median	3 rd Quartile	Stdev.	StdError	Max.	Unit
T1	91	175.0207	144.08	170.53	209.07	45.1389	8.6869	288.51	μs
T2	20.54	130.6507	52.285	116.41	190.995	90.4825	17.4134	349.23	μs
Frequency	4.719	4.9993	4.9195	5.003	5.0845	0.1339	0.0258	5.256	GHz
Anharmonicity	-0.34913	-0.34332	-0.345835	-0.3443	-0.34239	0.005597	0.001077	-0.31836	GHz
Readout assignment error	0.62	1.58259	0.82	1	1.47	1.81809	0.34989	9.92	×10 ⁻²
Prob. meas 0⟩ prep 1⟩	0.64	1.6229	1.01	1.14	1.38	1.73063	0.33306	9.74	×10 ⁻²
Prob. meas 1⟩ prep 0⟩	0.38	1.5423	0.64	0.84	1.69	1.9325	0.3719	10.1	×10 ⁻²
Readout length	817.778	817.778	817.778	817.778	817.778	0.0	0.0	817.778	ns
Single-qubit error	1.275	2.5334	1.7215	1.995	2.825	1.2913	0.2485		×10 ⁻⁴
CX Error	3.259	152.707	5.7327	8.8315	15.205	349.240	46.669	1000	×10 ⁻³
Gate time	181.333	384.571	283.555	344.889	464.889	138.187	18.466	728.889	ns

TABLE XXX: Summary of hardware performance, qubit characteristics and key specifications for the 27-qubit quantum computer *ibm_geneva*, featuring basis gates CX, ID, IF_ELSE, RZ, SX and X. The processor type is *Falcon r8*. The system boasts 56 CX qubit connections, and calibration data was accessed on November 14, 2022.

System characteristics	Min.	Mean	1 st Quartile	Median	3 rd Quartile	Stdev.	StdError	Max.	Unit
T1	52.81	299.6318	212.88	338.69	384.465	124.2378	23.90958	479.89	μs
T2	1.85	204.9359	108.215	202.21	300.63	126.6367	24.37123	458.16	μs
Frequency	4.55	4.6907	4.62	4.675	4.7485	0.09720	0.01870	4.88	GHz
Anharmonicity ^a	-	-	-	-	-	-	-	-	-
Readout assignment error	0.9	5.6267	1.56	3.38	5.105	8.5249	1.6406	42.54	×10 ⁻²
Prob. meas 0⟩ prep 1⟩	0.58	5.7215	1.89	3.34	5.12	8.5452	1.6445	41.2	×10 ⁻²
Prob. meas 1⟩ prep 0⟩	0.74	5.53185	1.41	2.62	5.65	8.62742	1.66035	43.88	×10 ⁻²
Readout length	1600	1600	1600	1600	1600	0.0	0.0	1600	ns
Single-qubit error	1.105	69.4995	1.8595	3.014	7.352	291.345	56.0695	1518	×10 ⁻⁴
CX Error	4.52	298	8.5007	16.250	1000	448.399	59.919	1000	×10 ⁻³
Gate time	348.444	588.698	462.222	558.223	695.111	170.282	22.755	988.444	ns

^a Missing values.

TABLE XXXI: Summary of hardware performance, qubit characteristics and key specifications for the 27-qubit quantum computer *ibmq_toronto*, featuring basis gates CX, ID, RZ, SX and X. The processor type is *Falcon r4*. The system boasts 56 CX qubit connections, and calibration data was accessed on November 14, 2022.

System characteristics	Min.	Mean	1 st Quartile	Median	3 rd Quartile	Stdev.	StdError	Max.	Unit
T1	50.99	117.58	97.535	118.66	141.3	36.7706	7.0765	188.87	μs
T2	12.53	125.5637	76.47	117.17	172.05	62.29247	11.98819	244.9	μs
Frequency	4.915	5.08025	5.0255	5.092	5.144	0.091117	0.017535	5.226	GHz
Anharmonicity	-0.33934	-0.32899	-0.336195	-0.33432	-0.32147	0.01130	0.002175	-0.28553	GHz
Readout assignment error	0.68	3.896296	1.635	2.31	5.25	3.67038	0.70637	15.66	×10 ⁻²
Prob. meas 0⟩ prep 1⟩	0.94	4.98963	2.43	3.72	7.45	3.87152	0.74507	17.9	×10 ⁻²
Prob. meas 1⟩ prep 0⟩	0.28	2.80296	0.6	0.98	3.16	3.84350	0.73969	13.42	×10 ⁻²
Readout length	5962.667	5962.667	5962.667	5962.667	5962.667	0.0	0.0	5962.667	ns
Single-qubit error	1.683	5.707	2.3915	3.076	3.912	8.46809	1.62969	40.90	×10 ⁻⁴
CX Error	6.1444	14.310	7.953	9.871	18.04	10.2225	0.012227	53.510	×10 ⁻³
Gate time	241.778	454.095	373.3335	451.5555	506.66675	126.725	16.934	860.444	ns

TABLE XXXII: Summary of hardware performance, qubit characteristics and key specifications for the 27-qubit quantum computer *ibm_peekskill*, featuring basis gates CX, ID, IF_ELSE, RZ, SX, X, X12, and XPRS. The processor type is *Falcon r8*. The system boasts 56 CX qubit connections, and calibration data was accessed on November 14, 2022.

System characteristics	Min.	Mean	1 st Quartile	Median	3 rd Quartile	Stdev.	StdError	Max.	Unit
T1	108.2	314.384	234.06	309.41	404.42	115.347	22.1986	533.37	μs
T2	122.41	297.613	196.24	283.69	394.055	124.5816	23.97574	589.01	μs
Frequency	4.627	4.949	4.8485	4.959	5.074	0.14096	0.27128	5.175	GHz
Anharmonicity	-0.38267	-0.34702	-0.34694	-0.34405	-0.34184	0.010515	0.002024	-0.33679	GHz
Readout assignment error	0.320	4.472	0.79	1.93	3.915	8.8130	1.6960	44.500	×10 ⁻²
Prob. meas 0⟩ prep 1⟩	0.24	3.777	0.77	1.68	3.81	6.6204	1.2741	34.40	×10 ⁻²
Prob. meas 1⟩ prep 0⟩	0.28	5.167	0.68	1.04	2.76	11.6171	2.2357	5.46	×10 ⁻²
Readout length	860.444	860.444	860.444	860.444	860.444	0.0	0.0	860.444	ns
Single-qubit error	0.7588	3.408	1.3535	1.695	3.0175	5.19027	0.99887	27.460	×10 ⁻⁴
CX Error	2.854	79.650	6.04775	7.12	10.46325	257.6373	34.42823	1000	×10 ⁻³
Gate time	291.556	472.889	398.222	451.5555	547.556	99.71249	13.32464	675.556	ns

TABLE XXXIII: Summary of hardware performance, qubit characteristics and key specifications for the 16-qubit quantum computer *ibmq_guadalupe*, featuring basis gates CX, ID, RZ, SX and X. The processor type is *Falcon* r4P. The system boasts 32 CX qubit connections, and calibration data was accessed on November 14, 2022.

System characteristics	Min.	Mean	1 st Quartile	Median	3 rd Quartile	Stdev.	StdError	Max.	Unit
T1	57.230	102.93	75.893	109.370	126.923	29.1918	7.2979	156.26	μs
T2	14.040	121.45	93.09	123.255	153	47.4965	11.8741	222.27	μs
Frequency	5.038	5.246	5.15475	5.2295	5.3215	0.1227	0.0307	5.470	GHz
Anharmonicity	-0.33734	-0.3272	-0.333956	-0.33096	-0.31743	0.00832	0.00207	-0.31579	GHz
Readout assignment error	0.980	1.955	1.3425	1.56	2.5025	0.9264	0.2316	4.160	×10 ⁻²
Prob. meas 0⟩ prep 1⟩	1.48	3.014	2.08	2.33	3.295	1.61999	0.40499	7.32	×10 ⁻²
Prob. meas 1⟩ prep 0⟩	0.340	0.896	0.5	0.69	1.02	0.57048	0.14262	2.46	×10 ⁻²
Readout length	7111.111	7111.111	7111.111	7111.111	7111.111	0.0	0.0	7111.111	ns
Single-qubit error	1.605	3.100	2.507	2.698	3.356	1.159	0.2898	5.692	×10 ⁻⁴
CX Error (32 connections)	6.017	10.520	7.803	8.805	12.890	3.7937	0.6706	17.700	×10 ⁻³
Gate time	263.111	416.4444	344.8885	384	378.222	122.9419	21.7333	775.111	ns

TABLE XXXIV: Summary of hardware performance, qubit characteristics and key specifications for the 7-qubit quantum computer *ibm_perth*, featuring basis gates CX, ID, IF_ELSE, RZ, SX and X. The processor type is *Falcon* r5.11H. The system boasts 12 CX qubit connections, and calibration data was accessed on November 13, 2022.

System characteristics	Min.	Mean	1 st Quartile	Median	3 rd Quartile	Stdev.	StdError	Max.	Unit
T1	90.63	143.24	111.295	127.84	175.23	45.363	17.145	211.16	μs
T2	53.13	112.964	86.23	98.39	141.18	45.922	17.357	184.41	μs
Frequency	4.863	5.068	5.0065	5.126	5.1575	0.114577	0.043330	5.159	GHz
Anharmonicity	-0.34727	-0.34192	-0.3452	-0.34152	-0.034045	0.004564	0.00175	-0.33337	GHz
Readout assignment error	0.65	1.69	1.18	1.20	1.78	1.17	0.44	4.09	×10 ⁻²
Prob. meas 0⟩ prep 1⟩	0.72	2.311	1.2	1.24	2.27	2.31	0.87	7.28	×10 ⁻²
Prob. meas 1⟩ prep 0⟩	0.58	1.077	0.89	1.12	1.22	0.3305	0.1249	1.62	×10 ⁻²
Readout length	675.556	675.556	675.556	675.556	675.556	0.0	0.0	675.556	ns
Single-qubit error	2.965	4.020	3.5	4.0	4.6	0.79	0.3	5.005	×10 ⁻⁴
CX Error	12.06	13.89	12.43	13.58	14.73	1.691	4.882	16.93	×10 ⁻³
Gate time	284.444	444.444	346.667	398.222	593.777	132.3611	38.2094	640	ns

TABLE XXXV: Summary of hardware performance, qubit characteristics and key specifications for the 7-qubit quantum computer *ibm_lagos*, featuring basis gates CX, ID, IF_ELSE, RZ, SX and X. The processor type is *Falcon* r5.11H. The system boasts 12 CX qubit connections, and calibration data was accessed on November 13, 2022.

System characteristics	Min.	Mean	1 st Quartile	Median	3 rd Quartile	Stdev.	StdError	Max.	Unit
T1	86.39	127.73	107.115	125.73	136.795	35.02391	13.23779	194.17	μs
T2	31.02	81.29857	57.145	86.10	95.235	38.40754	14.51669	147.21	μs
Frequency	4.987	5.147857	5.082	5.176	5.2115	0.1032818	0.039037	5.285	GHz
Anharmonicity	-0.34529	-0.34188	-0.343005	-0.34193	-0.34033	0.00210	0.000795	-0.33923	GHz
Readout assignment error	0.7	1.446	1.135	1.43	1.775	0.52430	0.19816	0.217	×10 ⁻²
Prob. meas 0⟩ prep 1⟩	0.78	1.651	1.37	1.76	1.89	0.58205	0.21999	2.5	×10 ⁻²
Prob. meas 1⟩ prep 0⟩	0.62	1.24	0.88	1.14	1.66	0.48826	0.184545	1.84	×10 ⁻²
Readout length	704	704	704	704	704	0	0	704	ns
Single-qubit error	1.647	2.758	2.0525	2.656	3.108	1.01898	3.851394	4.680	×10 ⁻⁴
CX Error(12 connections)	5.767	8.418	8.45	8.9875	9.135	1.2633	0.3647	9.182	×10 ⁻³
Gate time	256	359.111	296.889	327.111	341.333	113.272	32.699	611.556	ns

TABLE XXXVI: Summary of hardware performance, qubit characteristics and key specifications for the 7-qubit quantum computer *ibm_nairobi*, featuring basis gates CX, ID, IF_ELSE, RZ, SX and X. The processor type is *Falcon* r5.11H. The system boasts 12 CX qubit connections, and calibration data was accessed on November 13, 2022.

System characteristics	Min.	Mean	1 st Quartile	Median	3 rd Quartile	Stdev.	StdError	Max.	Unit
T1	50.59	118.86	111.95	117.71	140.235	35.09266	13.26377	159.35	μs
T2	22.72	101.59	60.995	85.62	116.565	73.53198	27.79247	247.63	μs
Frequency	5.027	5.19	5.1495	5.177	5.267	0.094361	0.035665	5.293	GHz
Anharmonicity	-0.34253	-0.34049	-0.3406	-0.3405	-0.3401	0.0011	0.0004	-0.3389	GHz
Readout assignment error	1.830	2.883	2.54	2.85	2.96	0.83	0.31	4.500	×10 ⁻²
Prob. meas 0⟩ prep 1⟩	2.9	4.117	3.36	4.4	4.64	0.93441	0.35317	5.52	×10 ⁻²
Prob. meas 1⟩ prep 0⟩	0.76	1.649	1.02	1.1	2.08	1.03	0.39	3.48	×10 ⁻²
Readout length	5560.889	5560.889	5560.889	5560.889	5560.889	0.0	0.0	5560.889	ns
Single-qubit error	1.674	2.805	2.3	2.8	3.4	0.79	0.3	3.768	×10 ⁻⁴
CX Error (12 connections)	6.177	11.77	7.622	9.172	1.749	5.740	1.6570	21.02	×10 ⁻³
Gate time	241.778	306.9629	275.5553	295.111	320	55.48440	16.01697	426.667	ns

TABLE XXXVII: Summary of hardware performance, qubit characteristics and key specifications for the 7-qubit quantum computer *ibm_oslo*, featuring basis gates CX, ID, IF_ELSE, RZ, SX and X. The processor type is *Falcon* r5.11H. The system boasts 12 CX qubit connections, and calibration data was accessed on November 13, 2022.

System characteristics	Min.	Mean	1 st Quartile	Median	3 rd Quartile	Stdev.	StdError	Max.	Unit
T1	57.14	116.93	79.98	128.85	131.76	51.08602	19.30869	209.04	μs
T2	31.32	78.8757	37.17	39.53	129.38	53.53095	20.23280	148.18	μs
Frequency	4.925	5.07771	4.9865	5.046	5.1405	0.135636	0.0512657	5.319	GHz
Anharmonicity	-0.3444	-0.34226	-0.34342	-0.329	-0.34203	0.00227	0.00086	-0.33763	GHz
Readout assignment error	1.040	4.31714	1.49	2.27	5.02	4.77287	1.80397	13.89	×10 ⁻²
Prob. meas 0⟩ prep 1⟩	1.06	4.2	1.42	2.64	4.85	4.432	1.675	13.16	×10 ⁻²
Prob. meas 1⟩ prep 0⟩	0.92	4.434285	1.41	2.20	5.24	5.12845	1.938373	14.62	×10 ⁻²
Readout length	910.222	910.222	910.222	910.222	910.222	0.0	0.0	910.222	ns
Single-qubit error	2.209	3.871	2.7	3.4	4.2	1.9	0.74	7.765	×10 ⁻⁴
CX Error	6.716	173.9	7.126	9.551	10.53	385.8677	111.3904	1000	×10 ⁻³
Gate time	167.111	300.44425	246.22225	320	341.333	75.37129	21.757817	412.444	ns

TABLE XXXVIII: Summary of hardware performance, qubit characteristics and key specifications for the 7-qubit quantum computer *ibmq_jakarta*, featuring basis gates CX, ID, IF_ELSE, RZ, SX and X. The processor type is *Falcon* r5.11H. The system boasts 12 CX qubit connections, and calibration data was accessed on November 13, 2022.

	Min.	Mean	1 st Quartile	Median	3 rd Quartile	Stdev.	StdError	Max.	Unit
T1	95.45	138.7942	116.46	136.5	161.105	32.734337	12.3724166	184.48	μs
T2	22.47	42.946	27.705	33.94	54.28	21.156	7.9964	80.24	μs
Frequency	5.014	5.1591	5.0855	5.143	5.219	0.0979	0.0346	5.301	GHz
Anharmonicity	-0.3432	-0.34067	-0.3415	-0.3411	-0.3396	0.0016	0.0005	-0.33836	GHz
Readout assignment error	1.610	2.590	2.07	2.7	3.02	0.71	8.55	3.640	×10 ⁻²
Prob. meas 0⟩ prep 1⟩	2.14	3.211	2.9	3.0	3.52	0.75	8.98	4.5	×10 ⁻²
Prob. meas 1⟩ prep 0⟩	1.06	1.969	1.24	1.62	2.16	1.16	0.44	4.3	×10 ⁻²
Readout length	5351.111	5351.111	5351.111	5351.111	5351.111	0.0	0.0	5351.111	ns
Single-qubit error	1.753	2.342	2.0	2.0	3.0	0.50	0.20	3.371	×10 ⁻⁴
CX Error	6.758	9.556	6.875	7.767	9.979	4.213078	1.216211	18.19	×10 ⁻³
Gate time	234.667	341.33333	275.55525	302.2225	392.889	100.0622	28.88546	540.444	ns

TABLE XXXIX: Summary of hardware performance, qubit characteristics and key specifications for the 5-qubit quantum computer *ibmq_manila*, featuring basis gates CX, ID, IF_ELSE, RZ, SX, and X. The processor type is *Falcon* r5.11H. The system boasts 8 CX qubit connections, and calibration data was accessed on November 13, 2022.

System characteristics	Min.	Mean	1 st Quartile	Median	3 rd Quartile	Stdev.	StdError	Max.	Unit
T1	102.52	137.296	129.47	132.79	152.995	25.12629	11.23682	168.75	μs
T2	23.23	57.92	70.58	40.69	70.58	29.46491	13.17711	100.37	μs
Frequency	4.838	4.9706	4.951	4.962	5.037	0.08855	0.0396	5.065	GHz
Anharmonicity	-0.34528	-0.34363	-0.34463	-0.34358	-0.34255	0.001342	0.0006	-0.34211	GHz
Readout assignment error	1.990	2.212	2.07	2.2	2.24	0.2187921	0.0978468	2.560	×10 ⁻²
Prob. meas 0⟩ prep 1⟩	2.94	3.332	3.1	3.36	3.4	0.351	3.332	3.86	×10 ⁻²
Prob. meas 1⟩ prep 0⟩	1.04	1.092	1.04	1.04	1.08	0.0954987	0.0427083	1.26	×10 ⁻²
Readout length	5351.111	5351.111	5351.111	5351.111	5351.111	0	0	5351.111	ns
Single-qubit error	2.335	2.829	2.4	2.5	2.6	0.9	0.4	4.436	×10 ⁻⁴
CX Error	7.053	8.156	7.1055	7.3705	8.421	1.666769	0.589292	10.83	×10 ⁻³
Gate time	277.333	368	309.3335	344.889	410.6665	81.85500	28.9401143	504.889	ns

TABLE XL: Summary of hardware performance, qubit characteristics and key specifications for the 5-qubit quantum computer *ibmq_quito*, featuring basis gates CX, ID, RZ, SX, and X. The processor type is *Falcon* r4T. The system boasts 8 CX qubit connections, and calibration data was accessed on November 13, 2022.

	Min.	Mean	1 st Quartile	Median	3 rd Quartile	Stdev.	StdError	Max.	Unit
T1	43.76	87.426	83.75	94.7	106.63	26.34978	11.78398	108.29	μs
T2	19.93	85.032	57.36	94.72	105.55	48.56339	21.71820	147.6	μs
Frequency	5.052	5.1838	5.081	5.164	5.3	0.123420	0.05520	5.322	GHz
Anharmonicity	-0.33508	-0.327478	-0.33232	-0.33148	-0.31926	0.007624	0.003409	-0.31925	GHz
Readout assignment error	3.510	4.430	3.58	3.58	3.99	1.721089	0.769695	7.490	×10 ⁻²
Prob. meas 0⟩ prep 1⟩	5.06	6.14	5.44	5.56	5.74	1.56	0.7	8.9	×10 ⁻²
Prob. meas 1⟩ prep 0⟩	1.42	2.72	1.46	1.72	2.92	1.98	0.88	6.08	×10 ⁻²
Readout length	5351.111	5351.111	5351.111	5351.111	5351.111	0	0	5351.111	ns
Single-qubit error	2.858	3.761	3.00	3.8	4.4	0.809867	0.36218	4.708	×10 ⁻⁴
CX Error	7.781	12.53	9.96275	11.755	14.3275	43.41329	1.534892	18.85	×10 ⁻³
Gate time	234.667	295.111	268.44425	288	318.22225	43.17165	15.26348	369.778	ns

TABLE XLI: Summary of hardware performance, qubit characteristics and key specifications for the 5-qubit quantum computer *ibmq_belem*, featuring basis gates CX, ID, RZ, SX, and X. The processor type is *Falcon* r4T. The system boasts 8 CX qubit connections, and calibration data was accessed on November 13, 2022.

System characteristics	Min.	Mean	1 st Quartile	Median	3 rd Quartile	Stdev.	StdError	Max.	Unit
T1	70.6	101	37.2	100.74	130.18	29.17987	13.04963	130.28	μs
T2	58.22	102.948	79.62	94.24	135.89	37.50387	16.77224	146.77	μs
Frequency	5.09	5.225	5.17	5.246	5.258	0.010158	0.04543	5.361	GHz
Anharmonicity	-0.33612	-0.329682	-0.33374	-0.33135	-0.33063	0.007641	0.003417	-0.31657	GHz
Readout assignment error	1.650	4.290	2.1	2.96	3.78	3.817185	1.707097	10.96	×10 ⁻²
Prob. meas 0⟩ prep 1⟩	2.96	7.428	3.28	4.74	6.16	7.142431	3.194193	20.0	×10 ⁻²
Prob. meas 1⟩ prep 0⟩	0.34	1.152	0.92	1.18	1.4	0.584226	0.261274	1.92	×10 ⁻²
Readout length	6158.222	6158.222	6158.222	6158.222	6158.222	0.00	0.00	6158.222	ns
Single-qubit error	1.735	26.1794	2.666	2.83	2.866	0.5289654	0.2365605	120.8	×10 ⁻⁴
CX Error	6.474	25.64	6.807	6.654	259.2925	458.93856	162.2593	1000	×10 ⁻³
Gate time	405.333	538.6666	433.77775	469.3335	588.44425	162.05814	57.29620	810.667	ns

TABLE XLII: Summary of hardware performance, qubit characteristics and key specifications for the 5-qubit quantum computer *ibmq_lima*, featuring basis gates CX, ID, RZ, SX, and X. The processor type is *Falcon* r4T. The system boasts 8 CX qubit connections, and calibration data was accessed on November 13, 2022.

System characteristics	Min.	Mean	1 st Quartile	Median	3 rd Quartile	Stdev.	StdError	Max.	Unit
T1	23.85	87.786	58.94	98.74	126.44	45.82035	20.49148	130.96	μs
T2	19.37	100.824	26.33	130.68	150.39	37.17569	32.72517	177.45	μs
Frequency	5.03	5.16	5.092	5.128	5.247	0.112434	0.05028	5.303	GHz
Anharmonicity	-0.33574	-0.33068	-0.33447	-0.3336	-0.33124	0.007085	0.003169	-0.31835	GHz
Readout assignment error	1.790	3.672	1.95	5.86	5.69	2.060903	0.921664	6.070	×10 ⁻²
Prob. meas 0⟩ prep 1⟩	2.52	5.2	3.04	4.18	8.82	3.314604	1.482336	9.54	×10 ⁻²
Prob. meas 1⟩ prep 0⟩	0.86	1.724	1.06	1.54	1.84	0.972358	0.434852	3.32	×10 ⁻²
Readout length	5351.111	5351.111	5351.111	5351.111	5351.111	0.0	0.0	5351.111	ns
Single-qubit error	4.736	7.642	5.723	6.948	9.381	2.734339	1.222834	11.42	×10 ⁻⁴
CX Error	6.318	12.49	7.58475	11.1335	16.0375	6.328578	2.237490	21.37	×10 ⁻³
Gate time	298.667	405.333	327.111	401.7775	487.1115	93.57069	33.08224	519.111	ns